THE ASTROPHYSICAL JOURNAL, 325:231–251, 1988 February 1

ACCRETION DISK MODELS FOR FU ORIONIS AND V1057 CYGNI: DETAILED COMPARISONS BETWEEN OBSERVATIONS AND THEORY[1]

S. J. KENYON,[2] L. HARTMANN,[2] AND R. HEWETT
Harvard-Smithsonian Center for Astrophysics
Received 1987 May 13; accepted 1987 July 23

ABSTRACT

We present further tests of the accretion disk hypothesis for FU Orionis objects. Steady disk models that fit the broad-band energy distributions of V1057 Cyg and FU Ori require accretion rates of $\dot{M} \sim 10^{-4}\ M_\odot\ \mathrm{yr}^{-1}$, which implies that $\sim 10^{-3}$ to $10^{-2}\ M_\odot$ is added to the central object during an FU Orionis eruption. These models make reasonably quantitative predictions regarding the shape of absorption-line profiles and variation of rotation with wavelength using a small number of free parameters. Our analysis of intermediate and high-resolution observations shows good agreement with theoretical disk spectra. We estimate that the central stars have masses and radii ($M_* \sim 0.3$–$1\ M_\odot$; $R_* \sim 4\ R_\odot$) appropriate for normal pre–main-sequence stars if the inclination of the disk's rotation axis to the line of sight is $i \lesssim 30°$ for V1057 Cyg and $25° \lesssim i \lesssim 70°$ for FU Ori.

The monotonic fading of brightness of V1057 Cyg in the optical and near-infrared provides strong support for the accretion model. The lack of decline at 4.8 μm cannot be accounted for by steady disks, but may be a consequence of time-dependent phenomena in the evolving disk. Material in the outer disk appears to reprocess radiation emitted by the inner disk, and is responsible for the substantial far-infrared decay at 10–20 μm.

Subject headings: spectrophotometry — stars: accretion — stars: individual (FU Ori, V1057 Cyg) — stars: pre–main-sequence

I. INTRODUCTION

In an earlier series of articles (Hartmann and Kenyon 1985, hereafter Paper I; Hartmann and Kenyon 1987*a*, *b*, hereafter Papers II and III), we argued that the outbursts of FU Orionis objects result from accretion of protostellar disk material onto a central T Tauri star. We showed that accretion disk models can account for many observed peculiarities of FU Orionis objects, and that plausible amounts of disk material can provide the necessary energy for outbursts on the required time scales.

The purpose of this paper is to test the accretion disk hypothesis further by comparing observations of FU Orionis objects with disk model predictions in additional quantitative detail. To this end we have computed high- and low-resolution theoretical accretion disk spectra, and have compared the results with corresponding observations of the two best studied objects, FU Ori and V1057 Cyg. A major focus of this paper is the analysis of high-dispersion line profiles. The synthetic disk spectra allow us to quantify the decrease of rotational line broadening with increasing wavelength of observation, a fundamental prediction of the disk hypothesis (Papers II and III).

We find ample support for the accretion disk model from our detailed analysis. A simple steady disk does remarkably well in accounting for the energy distribution, color evolution, spectral features, line profiles, and difference between optical and infrared rotation in V1057 Cyg. The simple disk model does less well for FU Ori, but still accounts for many observed features with a small number of adjustable parameters. Complicating factors, including rapid mass loss, time variability, and the absence of good spectral standards for low-temperature regions, probably account for many of the differences between theory and observation.

In § II we describe the observational data obtained for this program. The predictions of disk models for overall energy distributions and broad spectral features are compared with observation in § III. Analyses of high-resolution spectra are presented in § IV. The light curve of V1057 Cyg is discussed in the context of accretion disk evolution in § V. We discuss the significance of our results for accretion disk theory in § VI, and close with some general implications of our conclusions for early stellar evolution in § VII.

II. OBSERVATIONAL DATA

a) Infrared Photometry

Infrared data were obtained using standard filter sets available with the OTTO and HERMANN InSb photometric systems on the KPNO 1.3 m telescope on 1985 June 6–10, 1986 April 17–20, and 1986 October 12–14. The observations were made through broad-band filters at J (1.23 μm), H (1.66 μm), and K (2.22 μm); narrow-band filters (2.17 and 2.40 μm) were used to measure the CO index (CO = [2.40] − [2.17]). The data were corrected for atmospheric extinction using standard techniques, and were placed on the natural photometric system of each instrument by assuming that $K = H-K = J-K = \mathrm{CO} = 0$ for α Lyr. Reduced data were then transformed to the CIT system (Elias *et al.* 1982) as described by Kenyon (1988), and are listed in Table 1. Our estimated errors in the photometry are $\lesssim \pm 0.02$ mag.

[1] Research reported herein used the Multiple Mirror Telescope, a joint facility of the Smithsonian Institution and the University of Arizona.

[2] Visiting Astronomer, Kitt Peak National Observatory, National Optical Astronomy Observatories, which is operated by Associated Universities for Research in Astronomy, Inc., under contract with the National Science Foundation.

TABLE 1

INFRARED PHOTOMETRY OF V1057 CYG AND FU ORI

Object	JD	K	$H-K$	$J-K$	CO
V1057 Cyg	2,446,224	5.67	0.67	1.61	−0.03
	2,446,541	5.75	0.63	1.58	...
	2,446,717	5.72	0.63	1.55	0.01
FU Ori	2,446,717	4.90	0.48	1.24	0.08

b) Infrared Spectroscopy

Infrared spectroscopic observations of V1057 Cyg, FU Ori, and various standard stars were made on 1986 January 29–30 and September 18–19 with the 1.4 m Fourier transform spectrometer (FTS) at the coudé focus of the Mayall 4 m telescope. We obtained K-band spectra, concentrating on the region where the CO v'–v'' 2–0 and 3–1 vibrational bands appear. These data have an effective resolution of ~ 15 km s^{-1} after apodization (see Papers II and III for further discussion of the observations).

c) Optical Spectrophotometry

Low-resolution (10 Å) optical spectrophotometric data for V1057 Cyg and FU Ori were obtained in 1984–1986 with the cooled, dual-beam intensified Reticon scanner (IRS) mounted on the KPNO No. 1 and No. 2 90 cm telescopes. Simultaneous star and sky observations were made through two 25″ apertures separated by 1′, and the objects were periodically beam-switched to minimize differences between the two halves of the Reticon array. Additional observations of six to eight standard stars were made each night to place the data on the Hayes and Latham (1975) flux scale, and we estimate that resulting photometric calibration has an accuracy of $\pm 7\%$ for blue spectra (3500–6200 Å) and $\pm 5\%$ for red spectra (5800–8500 Å). The blue and red spectra agree to better than 5% in the region of overlap (5800–6200 Å), and have been merged into the spectra shown in Figure 1.

We have extracted broad-band B- and V-magnitudes and narrow-band continuum magnitudes, $m_\lambda = -2.5 \log F_\lambda - 21.1$, from the IRS data, and our results are listed in Table 2. The continuum bandpasses have widths of 30 Å and avoid strong absorption and/or emission features often found on spectra of peculiar objects. Our data are too noisy to estimate m_{3520} for V1057 Cyg; we estimate that the other magnitudes have accuracies of ± 0.05 mag at B and V, ± 0.07 mag at 3520 and 4500 Å, and ± 0.04 mag at 5550, 6370, and 7400 Å. The variation of ~ 0.4 mag observed at 3520 Å in FU Ori appears to be a real photometric change, but this object maintained nearly constant brightness at other wavelengths.

d) Optical Echelle Spectra

The echelle spectrographs and the intensified Reticon detectors of the MMT and the Whipple Observatory 1.5 m telescope on Mount Hopkins were used to obtain the optical data discussed here (see Latham 1982 and Papers I and II for additional details). The resolution of the data is roughly 12.5 km s^{-1} for both spectrographs. We concentrate on a single 50 Å echelle order centered near 6170 Å. We also briefly consider observations centered on an echelle order at 5200 Å taken with the same equipment.

III. COMPARISON OF DISK MODELS WITH LOW-RESOLUTION OBSERVATIONS

a) Steady Accretion Disk Models

We adopt the basic formalism for viscous accretion disks developed by Shakura and Sunyaev (1973, hereafter SS) and by Lynden-Bell and Pringle (1974, hereafter LBP). This model assumes that viscous shear between adjacent annuli within the disk is responsible for the transport of mass and angular momentum. The magnitude of the viscous stress is a free parameter in this theory, but if the accretion rate through the disk is *steady*, then the energy dissipated within a disk annulus is *independent* of the details of the viscosity (see LBP; SS). Observations suggest that the steady state assumption is a reasonable first approximation for disks in dwarf novae declining from maximum light (see, for example, Pringle, Verbunt, and Wade 1986; Cannizzo and Kenyon 1986, 1987; and refer-

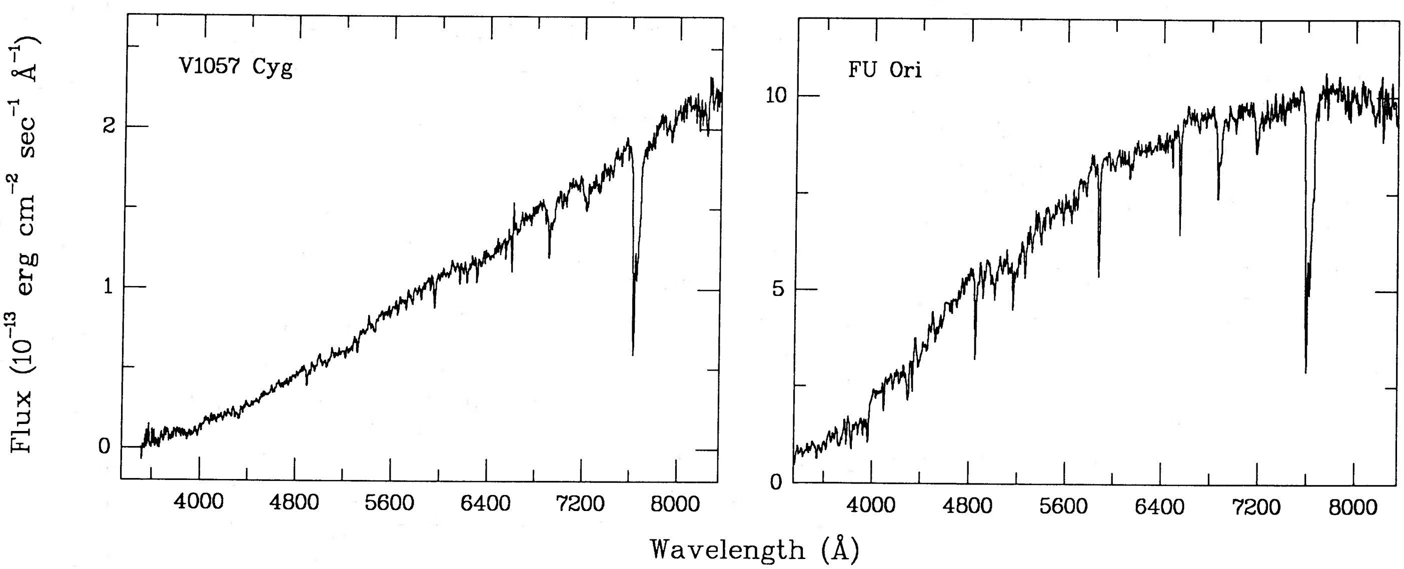

FIG. 1.—Optical spectra of V1057 Cyg and FU Ori. The data have *not* been corrected for interstellar reddening. Strong telluric absorption features are visible at 6800, 7200, and 7600 Å. Other features, including the P Cygni Hα emission-line profile, are intrinsic to FU Orionis objects, as described in the text.

TABLE 2

OPTICAL PHOTOMETRY OF V1057 CYG AND FU ORI

Object	JD	V	$B-V$	m_{3520}	m_{4500}	m_{5550}	m_{6370}	m_{7400}
V1057 Cyg	2,446,721	11.70	1.70	...	12.58	11.55	11.20	10.80
FU Ori	2,445,802	9.41	1.33	11.30	9.76	9.16	8.94	8.83
	2,445,984	...	...	...	...	...	8.89	8.80
	2,446,399	9.25	1.36	11.54	9.63	9.05	8.82	8.74
	2,446,721	9.23	1.38	11.70	9.65	9.04	8.88	8.77

ences therein), although steady disks provide a poor representation of the evolution from quiescence to light maximum in these short-period binaries. Thus, steady state disks should be a good approximation for the slow evolution of FU Orionis objects following visual maximum, but may not accurately portray the physical conditions in these objects *at* visual maxima.

The energy per unit surface area dissipated at radius R in a steady disk surrounding a star of mass M_* and radius R_* is

$$F_d(R) = \left(\frac{3GM_* \dot{M}}{8\pi R_*^3}\right)\left(\frac{R_*}{R}\right)^3\left[1 - \left(\frac{R_*}{R}\right)^{1/2}\right], \quad (1)$$

where $\dot{M}$ is the mass accretion rate through the disk onto the central star (SS; LBP). Making the usual assumption that $F_d(R)$ is radiated locally at the effective temperature, $T_d(R) = [F_d(R)/\sigma]^{1/4}$, equation (1) provides the variation of temperature with radius needed to synthesize the spectrum of a disk. The maximum disk temperature,

$$T_{\max} \approx 13{,}000\ \mathrm{K}\left(\frac{M_*}{1\ M_\odot}\right)^{1/4}\left(\frac{\dot{M}}{10^{-5}\ M_\odot\ \mathrm{yr}^{-1}}\right)^{1/4}\left(\frac{R_*}{R_\odot}\right)^{-3/4}, \quad (2)$$

occurs at $R_{\max} = 1.36\ R_*$ (LBP; Bath *et al.* 1974). Equation (1) implies that the disk temperature declines inside $R_{\max}$, and approaches zero near the stellar surface. This result is probably unrealistic; we assume that the inner annulus of the disk ($1.0\ R_* \leq R \leq 1.5\ R_*$) radiates the amount of energy required by equation (1) at a uniform temperature equal to $T_{\max}$.

As we noted in Paper I, the optical spectral type of an FU Orionis object is closely related to $T_{\max}$, and therefore fixes $M_*\ \dot{M}/R_*^3$ and the *shape* of the intrinsic energy distribution independent of any estimate for the optical extinction, A_V. Thus, a fit to the observed continuum flux distribution of an FU Orionis object with a disk model requires the same number of free parameters as would be used to fit the energy distribution with a stellar atmosphere model (a temperature, $T_{\max}$; a radius, R_*; and the extinction, A_V).

We synthesized disk spectra from 0.1 to 100 μm following the methods described in Paper I and in Canizzo and Kenyon (1986, 1987). The disk is divided into many concentric annuli, each of which radiates as a star with temperature T_d. The stellar spectrum libraries of Jacoby, Hunter, and Christian (1984) and Wu *et al.* (1983) provided optical and ultraviolet spectrophotometry for $T_d > 3500$ K; at lower temperatures we assumed blackbody energy distributions. The blackbody assumption provides a poor representation of the optical fluxes for the coolest annuli. This problem does not alter our conclusions, because such cool annuli contribute $\lesssim 10\%$ of the flux at optical wavelengths.

The vertical gravity component of the disk is not well determined, because it depends on the ratio of the photospheric height, H, to the radial distance, R, which in turn depends upon details of the vertical structure of the disk (and hence upon the poorly understood viscosity). Most disk models have $H/R \sim 0.1$ (see Herter *et al.* 1979; Mayo, Wickramasinghe, and Whelan 1980). This ratio implies gravities of log $g \sim 1$ for the portions of the disk which dominate the optical spectrum, assuming a central mass $\sim 0.5\ M_\odot$. We therefore used supergiants to model the disk spectrum.

Limits on the radius of the accreting star, R_*, and the inclination of the disk to the line of sight, i, can be derived from the dereddened visual magnitude once $T_{\max} \sim (M_*\ \dot{M}/R_*^3)^{1/4}$ has been chosen to fit the observed energy distribution. The apparent visual magnitude of a disk at a distance d is

$$V = V_0(T_{\max}) + 5\log\left(\frac{d}{10\ \mathrm{pc}}\right) - 5\log\left(\frac{R_*}{R_\odot}\right) - 2.5\log(\cos i)\,, \quad (3)$$

where $V_0(T_{\max})$ is the visual magnitude of a disk with $R_* = 1\ R_\odot$ at $d = 10$ pc viewed along the disk's rotation axis ($i = 0°$). Thus, an estimate for $(R_*/R_\odot)^2 \cos i$ can be obtained if $T_{\max}$ and d are known.

b) Broad-Band Energy Distributions

The starting point for testing the disk model is the dereddened energy distribution. The optical and infrared data in Tables 1 and 2 have been supplemented with *IUE* spectra (FU Ori: Ewald, Imhoff, and Giampapa 1986), optical photometry (FU Ori: Lee 1970; V1057 Cyg: $V-I$ from Kopatskaya 1984), IR photometry (FU Ori: Low 1970; Cohen 1973*b*; Mould *et al.* 1978; V1057 Cyg: Simon *et al.* 1982), and infrared data for FU Ori from the *IRAS Point Source Catalog* (1985). The resulting broad-band flux distributions for V1057 Cyg and FU Ori have been corrected for extinction using a standard reddening law (Savage and Mathis 1979).

As shown in Figure 2, accretion disk models with $T_{\max} = 7200$ K (FU Ori) and $T_{\max} = 6580$ K (V1057 Cyg) adequately reproduce the energy distributions between $\sim$4000 Å and 10 μm (Paper I). The choice of $T_{\max}$ depends somewhat upon the amount of extinction adopted; changes of $\sim$400 K from these values can be accommodated with reasonable variations of A_V (see § III*c* below). Standard stars fail to reproduce the infrared excess by a large margin. Pure accretion disk models do not account for the excess IR emission seen at $\lambda \gtrsim 20\ \mu$m. In § III*e* we argue that the long-wavelength excess in V1057 Cyg is probably produced by distant dust reradiating absorbed optical light, rather than accretion. We also show that the outer regions of a flaring disk (a disk whose thickness proportionately increases with increasing radial distance) could account for this reprocessing component.

If we adopt a distance of $d = 550$–650 pc for V1057 Cyg, then the observed $V = 11.7$ implies $(R_*/R_\odot)^2 \cos i \sim 10$–$20$ for

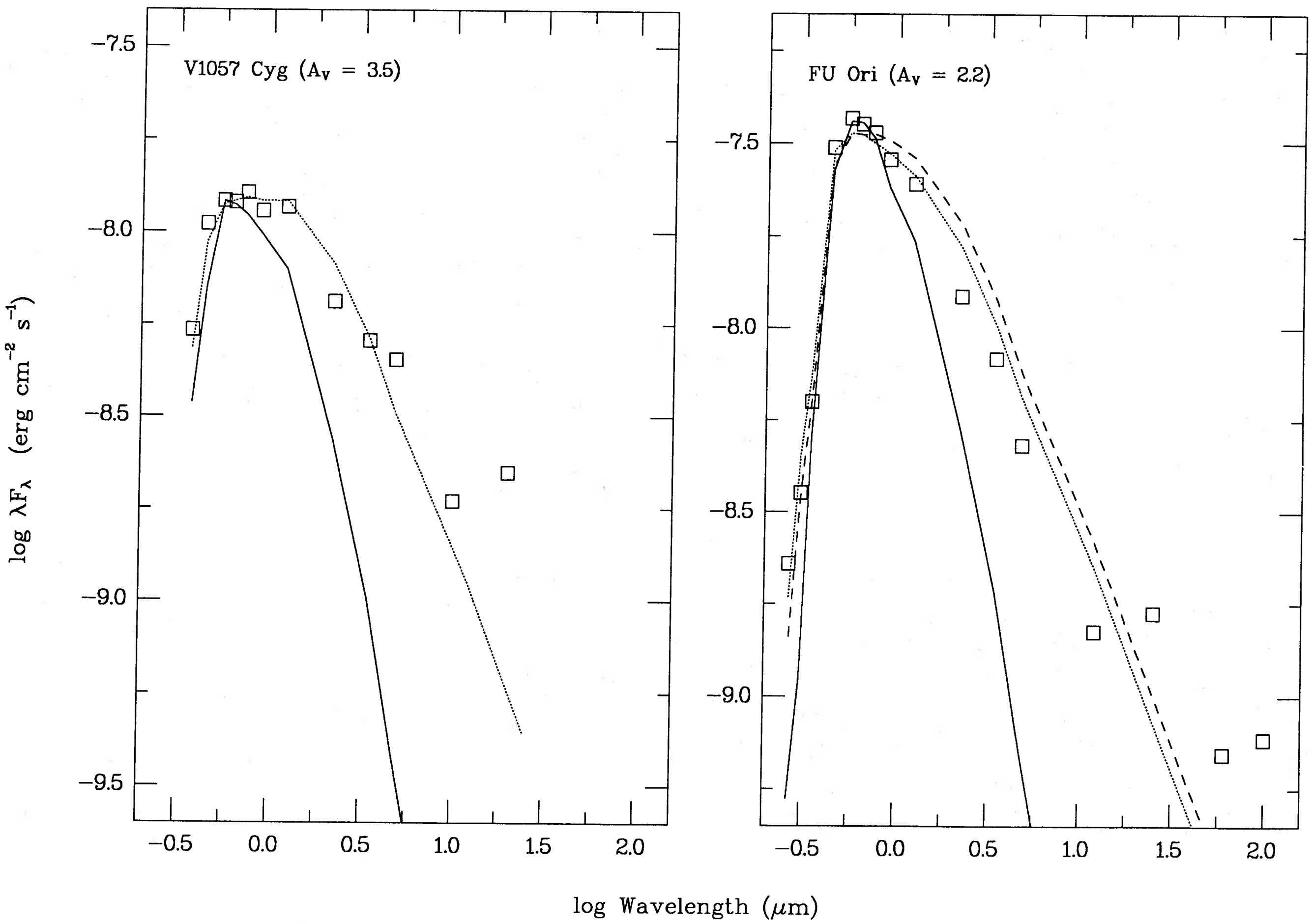

FIG. 2.—Broad-band energy distributions of FU Orionis objects compared with accretion disk models. Open squares denote observed fluxes corrected for interstellar extinction using the Savage and Mathis (1979) reddening law and the visual excess given in the legend. Dotted lines denote fluxes computed for the accretion disk models given in Tables 3 and 4 for V1057 Cyg and FU Ori, respectively. The dashed line in the right-hand panel indicates a second disk model for FU Ori with a maximum temperature 400 K cooler than that given in Table 4. The solid lines in each figure are energy distributions for standard G supergiants. Sources of the photometric data for V1057 Cyg and FU Ori are given in the text. The V1057 Cyg data represent the present epoch.

$A_V = 3.5 \pm 0.5$ mag. We derive $(R_*/R_\odot)^2 \cos i \sim 10$–20 in FU Ori for $V = 9.3$, $A_V = 1.85 \pm 0.5$ mag, and $d = 450$–550 pc. If $\cos i \sim \frac{1}{2}$, the radius of the central star would be $R_* \sim 4.5$–6.5 $R_\odot$, comparable to that expected for pre–main-sequence T Tauri stars (Cohen and Kuhi 1979). This radius estimate results in $M_* \dot{M} \sim (0.5\text{–}3) \times 10^{-4}\ M_\odot^2\ \mathrm{yr}^{-1}$ for V1057 Cyg and $M_* \dot{M} \sim (0.5\text{–}4) \times 10^{-4}\ M_\odot^2\ \mathrm{yr}^{-1}$ for FU Ori.

Basic parameters concerning individual disk annuli for V1057 Cyg and FU Ori models are summarized in Tables 3 and 4. The first three columns of these tables list the spectral type ("BB" denotes a blackbody stellar spectrum), outer radius (in units of R_*), and effective temperature for each annulus, while additional columns present the fraction each annulus contributes to the flux at various wavelengths. The column labeled "Total" represents the fraction of bolometric luminosity radiated by each annulus. Note that the inner radius of the first annulus is at $R/R_* = 1$. As described in § IV below, high-resolution optical spectra are used to determine $v \sin i$ [equivalent to $(M_*/R_*)^{1/2} \sin i$] at the inner edge of the disk for each FU Orionis object. Values for $v \sin i$ at the inner radius of the disk are given in the notes to Tables 3 and 4.

c) *Optical Spectral Energy Distributions*

The energy distributions shown in Figure 2 suggest that the observations and the disk model exhibit a short-wavelength excess of radiation relative to standard stars. We use the IRS spectra to examine this region in more detail, correcting for reddening using Schild's (1977) extinction law. To display the deviations of the object energy distributions from normal stellar photospheric fluxes, we have divided the resulting spectra by F and G standard stars obtained with the same instrument (Jacoby, Hunter, and Christian 1984).

In Figure 3 we display the IRS spectrum of V1057 Cyg divided by three standard stars and our disk model. The V1057 Cyg data have been dereddened by varying amounts to flatten the 6000–7400 Å region. It is apparent that G4–G5 stars are a good match to the red continuum for $A_V \sim 3.5$–4, but fail at shorter wavelengths, where V1057 Cyg has a large blue excess, as emphasized by Herbig (1977). The situation is not helped by choosing different spectral type standards; one is unable to flatten the spectrum throughout the wavelength interval 4000–7400 Å. Large departures from standard reddening laws would

TABLE 3

Disk Model for V1057 Cyg

Sp Type		Radius	Temp	Fractional Fluxes as a Function of Wavelength in Microns										
				0.27	0.35	0.45	0.55	0.64	0.74	0.90	1.25	2.20	3.50	Total
F6	I	1.50	6590.	0.63	0.40	0.31	0.21	0.16	0.13	0.12	0.08	0.03	0.02	0.08
F7	I	1.73	6370.	0.12	0.12	0.15	0.14	0.12	0.11	0.08	0.05	0.02	0.01	0.05
F8	I	1.95	6150.	0.13	0.19	0.14	0.12	0.10	0.09	0.07	0.05	0.02	0.01	0.05
G0	I	2.14	5800.	0.04	0.07	0.09	0.09	0.09	0.08	0.06	0.04	0.02	0.01	0.04
G1	I	2.26	5650.	0.02	0.04	0.04	0.04	0.04	0.04	0.03	0.02	0.01	0.01	0.02
G2	I	2.37	5500.	0.02	0.02	0.03	0.04	0.04	0.04	0.03	0.02	0.01	0.01	0.02
G3	I	2.55	5370.	0.03	0.04	0.04	0.05	0.05	0.04	0.04	0.03	0.01	0.01	0.03
G5	I	2.77	5100.	0.01	0.03	0.04	0.05	0.05	0.04	0.04	0.03	0.02	0.01	0.03
K0	I	2.98	4900.	0.	0.01	0.02	0.03	0.04	0.03	0.03	0.02	0.01	0.01	0.03
K1	I	3.20	4700.	0.	0.01	0.02	0.03	0.03	0.03	0.03	0.03	0.01	0.01	0.03
K2	I	3.85	4500.	0.	0.03	0.06	0.07	0.08	0.08	0.08	0.07	0.04	0.02	0.07
K5	I	4.60	3750.	0.	0.01	0.03	0.05	0.07	0.08	0.10	0.11	0.08	0.05	0.06
M1	I	4.86	3600.	0.	0.01	0.01	0.01	0.02	0.02	0.03	0.03	0.03	0.02	0.02
M2	I	5.19	3500.	0.	0.01	0.01	0.02	0.02	0.03	0.04	0.04	0.04	0.02	0.02
BB		5.70	3300.	0.	0.01	0.01	0.02	0.02	0.03	0.04	0.05	0.04	0.02	0.03
BB		6.28	3100.	0.	0.	0.	0.01	0.02	0.03	0.04	0.05	0.04	0.03	0.03
BB		6.96	2900.	0.	0.	0.	0.01	0.02	0.03	0.03	0.05	0.04	0.03	0.03
BB		7.77	2700.	0.	0.	0.	0.01	0.01	0.02	0.03	0.04	0.05	0.03	0.03
BB		8.73	2500.	0.	0.	0.	0.	0.01	0.02	0.02	0.04	0.05	0.04	0.03
BB		9.91	2300.	0.	0.	0.	0.	0.	0.01	0.02	0.04	0.06	0.05	0.03
BB		11.37	2100.	0.	0.	0.	0.	0.	0.01	0.01	0.03	0.06	0.05	0.03
BB		13.22	1900.	0.	0.	0.	0.	0.	0.	0.01	0.03	0.06	0.06	0.03
BB		15.64	1700.	0.	0.	0.	0.	0.	0.	0.01	0.02	0.06	0.07	0.02
BB		18.89	1500.	0.	0.	0.	0.	0.	0.	0.	0.01	0.06	0.08	0.02
BB		23.46	1300.	0.	0.	0.	0.	0.	0.	0.	0.01	0.05	0.08	0.02
BB		28.16	1100.	0.	0.	0.	0.	0.	0.	0.	0.	0.03	0.06	0.02
BB		32.35	1000.	0.	0.	0.	0.	0.	0.	0.	0.	0.01	0.04	0.01
BB		37.74	900.	0.	0.	0.	0.	0.	0.	0.	0.	0.01	0.04	0.01
BB		44.86	800.	0.	0.	0.	0.	0.	0.	0.	0.	0.01	0.03	0.01
BB		54.64	700.	0.	0.	0.	0.	0.	0.	0.	0.	0.	0.03	0.01
BB		68.77	600.	0.	0.	0.	0.	0.	0.	0.	0.	0.	0.02	0.01
BB		90.64	500.	0.	0.	0.	0.	0.	0.	0.	0.	0.	0.01	0.01
BB		128.19	400.	0.	0.	0.	0.	0.	0.	0.	0.	0.	0.	0.01
BB		204.84	300.	0.	0.	0.	0.	0.	0.	0.	0.	0.	0.	0.01
BB		429.26	200.	0.	0.	0.	0.	0.	0.	0.	0.	0.	0.	0.01

Note.—$v \sin i$ ($R = 1$) = 42.6 km s^{-1}. Because of rounding errors the sum of the fractional fluxes in a given column may not be identically equal to unity.

be required to correct the optical continuum to match that of a G supergiant from 4000 to 7400 Å.

The amount of blue excess in V1057 Cyg is smaller when compared with giant and main-sequence standard stars, but division by high-gravity standards creates a pronounced ripple in the spectrum between ~4500 and 5500 Å. It is unlikely that this feature is an artifact of the interstellar reddening law. We suggest instead that the shape of the spectral divisions indicates low atmospheric gravities for FU Orionis objects (see also Paper I), consistent with optical spectral types derived from higher resolution data (Herbig 1966, 1977).

The disk model provides a reasonable representation of the optical continuum for V1057 Cyg if $A_V = 3.5$ mag. There is some evidence for the "4800 Å ripple" in the divided spectra shown in Figure 3. Because the ripple decreases in intensity with decreasing gravity, the observations suggest that V1057 Cyg has a lower gravity than that of the normal supergiants used to construct the disk model.

The spectral analysis is more complicated for FU Ori, because this object appears to be variable below 4000 Å. In Figure 4 we show two divided spectra of FU Ori using data from a third epoch (1985 November) as the reference spectrum. The spectra are nearly identical for $\lambda > 4000$ Å, except for a small zero-point offset of ~0.05 mag, but they deviate significantly at shorter wavelengths. Although the spectra are very noisy in the blue, the 1984 April spectrum shows a small (~0.15 mag) excess over the 1985 November data at 3500 Å, while the 1986 October spectrum has a slight deficit of radiation below 4000 Å. It does not seem likely that these variations result from a poor photometric calibration in the blue, because repeated observations of bright objects agree to within ±0.05 mag at 3500 Å while the various FU Ori observations disagree by ~0.3–0.4 mag at this wavelength. However, it is possible that small fluctuations in sky transparency could produce the observed effect in FU Ori without affecting results for brighter objects. Given these complications, we restrict our analysis of FU Ori to $\lambda > 4000$ Å.

It may be that the fluctuations below 4000 Å in FU Ori are related to the possibly periodic variability reported by Kolotilov and Petrov (1985), but our observations are not extensive enough to test this hypothesis.

The ratios of the FU Ori energy distribution to those of standard stars shown in Figure 5 are similar to those presented in Figures 2–3 of Paper I. As with V1057 Cyg, the prominent blue excess which FU Ori displays over a G0 supergiant can be reduced if higher gravity stars are used as standards, but this procedure introduces the 4500–5500 Å ripple in the divided spectra.

The spectrum of FU Ori divided by the synthetic spectrum of our standard disk model ("model A"; see Table 4) is not

TABLE 4

DISK MODEL FOR FU ORI

Sp	Type	Radius	Temp	Fractional Fluxes as a Function of Wavelength in Microns										
				0.27	0.35	0.45	0.55	0.64	0.74	0.90	1.25	2.20	3.50	Total
F2	I	1.46	7200.	0.33	0.23	0.23	0.17	0.14	0.12	0.09	0.06	0.03	0.01	0.08
F3	I	1.61	7065.	0.19	0.15	0.11	0.08	0.07	0.05	0.05	0.03	0.01	0.01	0.04
F4	I	1.71	6930.	0.12	0.09	0.07	0.05	0.04	0.03	0.03	0.02	0.01	0.01	0.02
F5	I	1.83	6800.	0.12	0.08	0.07	0.06	0.05	0.04	0.03	0.02	0.01	0.01	0.03
F6	I	1.98	6590.	0.11	0.11	0.09	0.07	0.06	0.05	0.04	0.03	0.01	0.01	0.03
F7	I	2.14	6370.	0.03	0.05	0.07	0.07	0.07	0.06	0.04	0.03	0.01	0.01	0.03
F8	I	2.35	6150.	0.05	0.11	0.09	0.08	0.08	0.07	0.06	0.04	0.02	0.01	0.04
G0	I	2.54	5800.	0.02	0.04	0.06	0.07	0.07	0.07	0.05	0.04	0.02	0.01	0.03
G1	I	2.67	5650.	0.01	0.03	0.03	0.03	0.04	0.03	0.03	0.02	0.01	0.01	0.02
G2	I	2.80	5500.	0.01	0.01	0.02	0.03	0.03	0.03	0.02	0.02	0.01	0.01	0.02
G3	I	2.99	5370.	0.01	0.02	0.03	0.04	0.04	0.04	0.03	0.03	0.01	0.01	0.03
G5	I	3.23	5100.	0.	0.02	0.03	0.04	0.04	0.04	0.04	0.03	0.02	0.01	0.03
K0	I	3.46	4900.	0.	0.01	0.02	0.03	0.03	0.03	0.03	0.02	0.01	0.01	0.03
K1	I	3.71	4700.	0.	0.01	0.02	0.02	0.03	0.03	0.03	0.02	0.01	0.01	0.03
K2	I	4.43	4500.	0.	0.02	0.04	0.06	0.07	0.07	0.07	0.06	0.04	0.02	0.06
K5	I	5.28	3750.	0.	0.01	0.02	0.04	0.05	0.07	0.09	0.10	0.08	0.05	0.06
M1	I	5.56	3600.	0.	0.	0.	0.01	0.01	0.02	0.03	0.03	0.03	0.02	0.02
M2	I	5.94	3500.	0.	0.	0.	0.01	0.02	0.03	0.04	0.04	0.03	0.02	0.02
BB		6.51	3300.	0.	0.	0.	0.01	0.02	0.03	0.04	0.04	0.04	0.02	0.03
BB		7.16	3100.	0.	0.	0.	0.01	0.02	0.03	0.03	0.04	0.04	0.03	0.03
BB		7.93	2900.	0.	0.	0.	0.01	0.01	0.02	0.03	0.04	0.04	0.03	0.03
BB		8.84	2700.	0.	0.	0.	0.	0.01	0.02	0.03	0.04	0.05	0.03	0.02
BB		9.93	2500.	0.	0.	0.	0.	0.01	0.01	0.02	0.04	0.05	0.04	0.02
BB		11.26	2300.	0.	0.	0.	0.	0.	0.01	0.02	0.04	0.05	0.05	0.02
BB		12.90	2100.	0.	0.	0.	0.	0.	0.01	0.01	0.03	0.06	0.05	0.02
BB		14.99	1900.	0.	0.	0.	0.	0.	0.	0.01	0.02	0.06	0.06	0.02
BB		17.71	1700.	0.	0.	0.	0.	0.	0.	0.	0.02	0.06	0.07	0.02
BB		21.38	1500.	0.	0.	0.	0.	0.	0.	0.	0.01	0.06	0.08	0.02
BB		26.54	1300.	0.	0.	0.	0.	0.	0.	0.	0.01	0.05	0.08	0.02
BB		31.83	1100.	0.	0.	0.	0.	0.	0.	0.	0.	0.03	0.06	0.01
BB		36.56	1000.	0.	0.	0.	0.	0.	0.	0.	0.	0.01	0.04	0.01
BB		42.63	900.	0.	0.	0.	0.	0.	0.	0.	0.	0.01	0.04	0.01
BB		50.66	800.	0.	0.	0.	0.	0.	0.	0.	0.	0.01	0.03	0.01
BB		61.68	700.	0.	0.	0.	0.	0.	0.	0.	0.	0.	0.02	0.01
BB		77.59	600.	0.	0.	0.	0.	0.	0.	0.	0.	0.	0.02	0.01
BB		102.23	500.	0.	0.	0.	0.	0.	0.	0.	0.	0.	0.01	0.01
BB		144.53	400.	0.	0.	0.	0.	0.	0.	0.	0.	0.	0.	0.01
BB		230.84	300.	0.	0.	0.	0.	0.	0.	0.	0.	0.	0.	0.01
BB		483.49	200.	0.	0.	0.	0.	0.	0.	0.	0.	0.	0.	0.01

NOTE.—$v \sin i$ $(R = 1) = 93$ km s^{-1}. Because of rounding errors the sum of the fractional fluxes in a given column may not be identically equal to unity.

much flatter than divisions by dwarfs. At higher resolution FU Ori exhibits spectral features which identify it as a low-gravity object (Herbig 1966), so comparison with the supergiant spectrum is probably more relevant. Although the disk model does a better job of reproducing the overall energy distribution of FU Ori than does the supergiant, the large hump in the division is worrisome, as is the mismatch in G-band strength (λ4300). Disk model B, which has a lower maximum temperature ($T_{max} = 6800$ K instead of 7200 K) and therefore exhibits a "later" average spectrum, provides a slightly better match to FU Ori. However, as shown in Figure 2, model B also produces a larger infrared excess than model A, resulting in poorer agreement at long wavelengths.

When trying to match the object spectrum with a theoretical model at a level of $\lesssim 20\%$, one must consider the effects of at least three complicating factors: the details of the extinction law; the limb-darkening properties of a flat disk atmosphere; and the effects of extra line blanketing in the massive wind. We briefly consider these three effects below.

Slight departures from a normal extinction law can make sizable changes in the broad-band flux distributions of heavily reddened objects such as FU Ori. Herbig (1966) noted that the diffuse interstellar bands expected to be present in normal regions with $E_{B-V} \sim 0.8$ are not observed in FU Ori, suggesting that the intervening material may not have "standard" properties. We estimate the changing $R = A_V/E_{B-V}$ from 3.1 to ~ 3.5 would bring model B into much better agreement with the broad-band photometry.

The fluxes from standard stars used in the spectrum synthesis correspond to an integral of fluxes over the stellar surface, or, equivalently, to the flux integral over angle in the limit of plane-parallel atmospheres. In contrast, the flux from a flat disk is an integral over the disk of fluxes at the same angle of inclination. Therefore, limb darkening will have different effects on a disk spectrum than on a stellar spectrum, and in particular the shape of the spectrum from a disk will vary as a function of viewing angle.

To get some idea of the size of this effect in the optical regions, we examine the emergent radiation from a simple $T_{eff} = 5000$ K, $\log g = 2$ model atmosphere from Carbon and Gingerich (1969). The solid and dashed lines at the bottom of Figure 5 indicate the relative intensities of this atmosphere at two inclination angles. These intensities have been divided by the flux integral for the atmosphere as a function of wave-

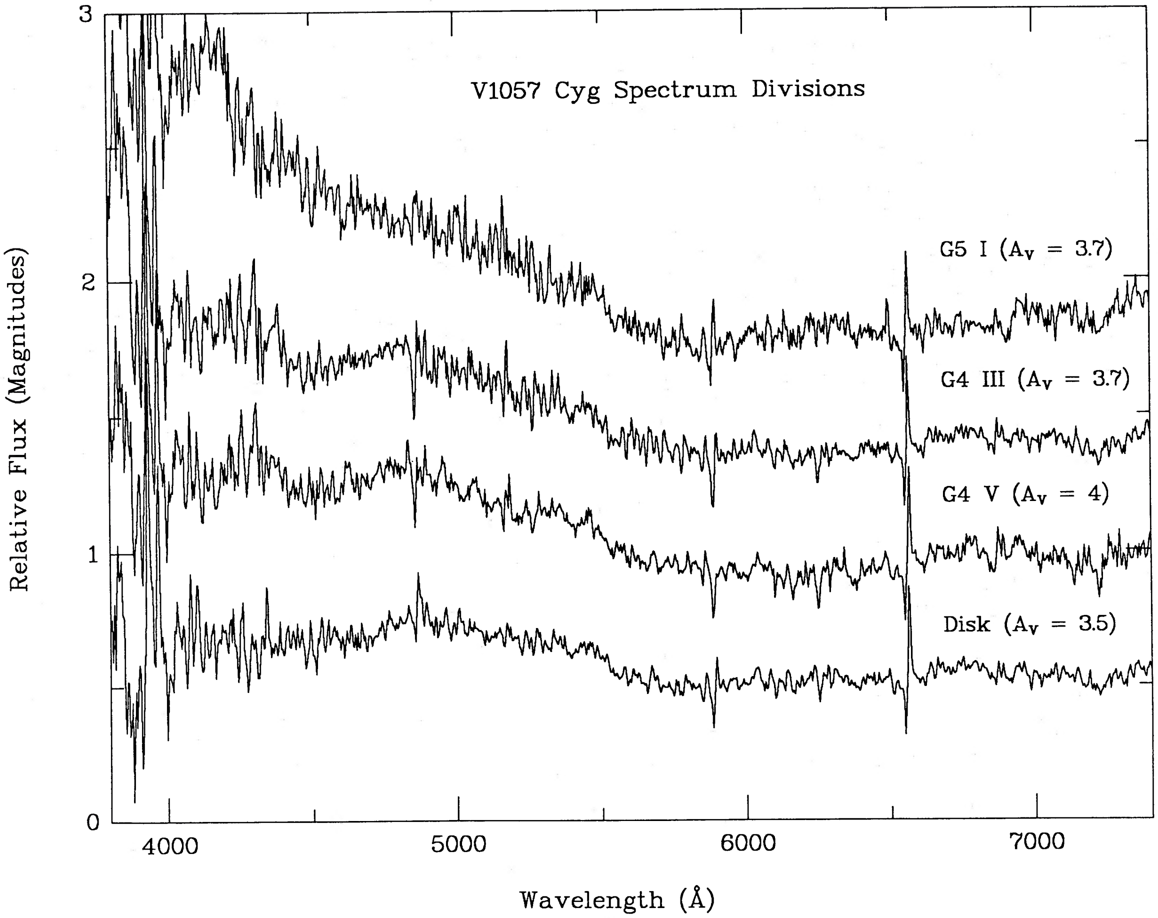

FIG. 3.—IRS spectrum of V1057 Cyg in Fig. 1 divided by spectra of standard G5 I, G4 III, and G4 V stars from the spectral atlas of Jacoby, Hunter, and Christian (1984), and divided by the energy distribution for the disk model of Table 3. Different extinction corrections, as labeled above each curve, have been applied to each spectrum division to flatten the result between ~5500 and 7400 Å. V1057 Cyg has a large blue excess relative to a supergiant standard which approximately matches the optical spectral type (Herbig 1977). The disk model, which uses a sequence of supergiant spectra, is able to reproduce the blue excess much more satisfactorily. The division is poor at Hα, Hβ, and Na I, which are strongly affected by mass loss in V1057 Cyg, and chromospheric emission at Ca II H and K is noticeable.

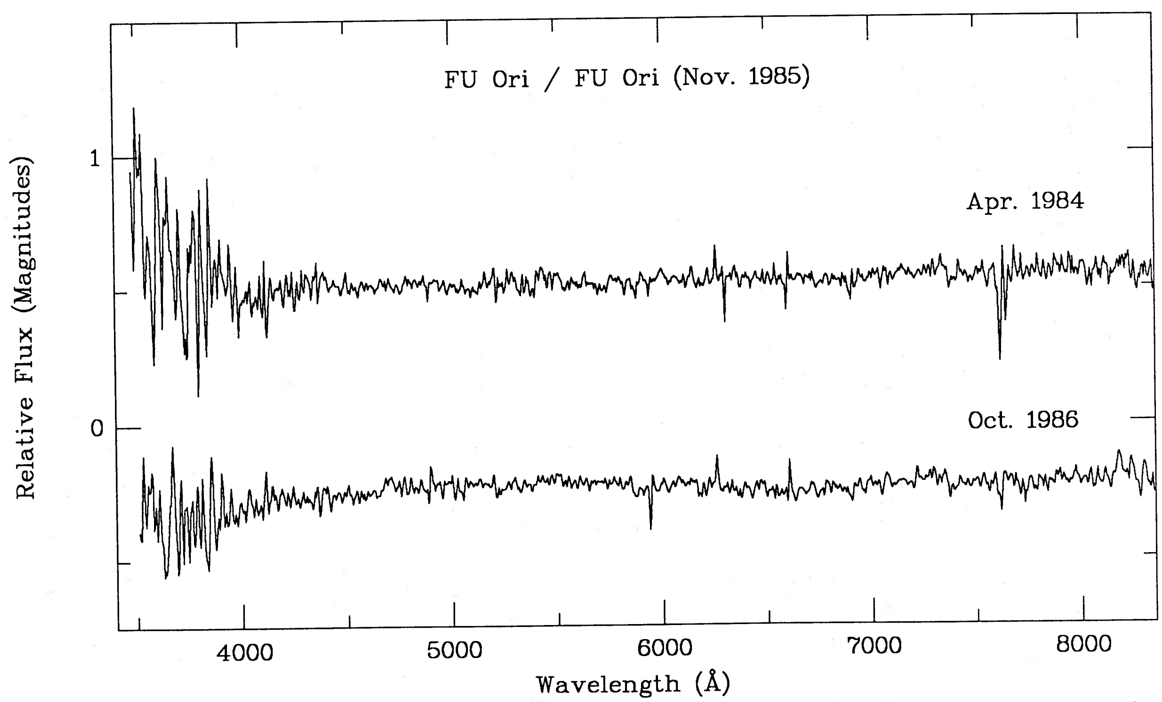

FIG. 4.—IRS spectra of FU Ori in 1984 April and 1986 October divided by a 1985 November spectrum. Substantial variability below 4000 Å is evident.

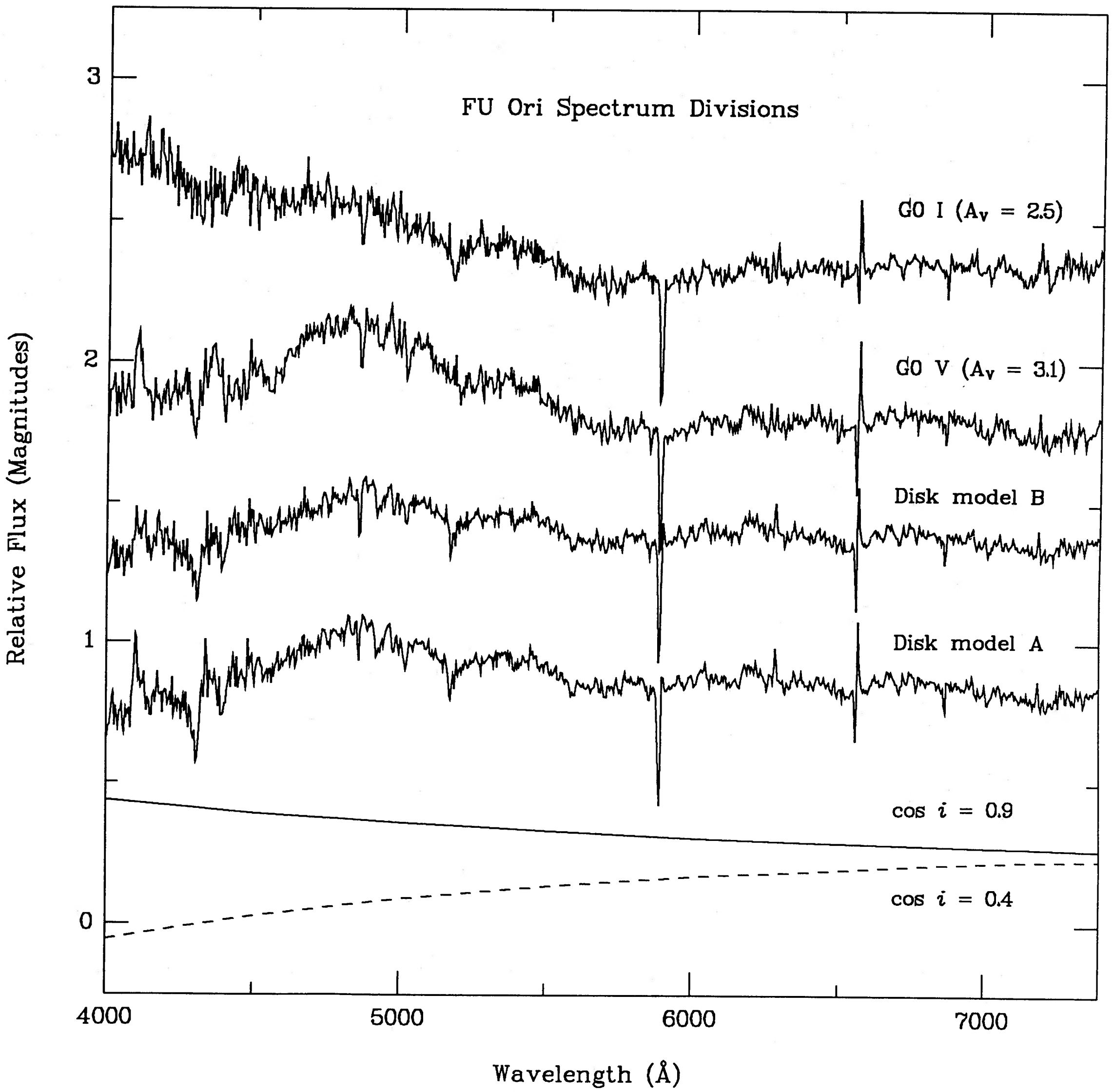

FIG. 5.—IRS spectrum of FU Ori from Fig. 1 divided by various standard stars and disk models. Division by a G supergiant, consistent with Herbig's (1966, 1977) spectral type, results in a substantial blue excess. Disk model A (Table 4, corresponding to the dotted line in the right-hand panel Fig. 2) better matches the blue excess, but division by this model energy distribution results in a downturn below 5000 Å, and has far less G-band absorption (λ4300) than observed. Disk model B, which has a slightly lower maximum temperature, flattens the spectrum division somewhat more adequately, and reduces the mismatch at the G band, but produces a larger infrared excess (dashed line in right-hand panel of Fig. 2). The effects of mass loss in FU Ori account for poor divisions at the Hα, Hβ, Na I, and Mg I λ5180 lines. The solid and dashed lines at the bottom of this figure show the variation of flux (relative to 8000 Å) emitted by a plane-parallel atmosphere as a function of wavelength for the two different viewing angles listed in the legend. Limb darkening causes the gradual decline in relative flux at small cos i, and may be responsible for similar behavior observed in the FU Ori spectrum divisions.

length, and normalized to unity at 8000 Å. One observes that for disks observed nearly pole-on, the limb-darkening effect is not large, but more nearly edge-on disks might have a significant downturn in the energy distribution, which becomes larger at shorter wavelengths.

In § VI*c* we suggest that FU Ori is likely to be less pole-on as seen from Earth than V1057 Cyg. Thus part of the downturn seen in the disk spectral division shown in Figure 5 may result from limb-darkening effects ignored in our simple modeling.

Neither extinction nor limb darkening can account for the obvious mismatch between observation and model seen in some spectral lines. FU Ori obviously has stronger G-band and Mg I *b* absorption than the model. Herbig (1966) noted the presence of strong "shell" lines in FU Ori, displaced blueward of the underlying stellar spectrum by 50–80 km s^{-1}. These shell features are especially prominent in low-excitation lines of Fe, Ti, and Ca, producing what Herbig called a "second" spectrum of roughly G supergiant type. The shell lines are almost certainly formed in the strong wind that emanates from FU Ori (e.g., Bastian and Mundt 1985; Croswell, Hartmann, and Avrett 1987). The shell features may produce extra line blanketing, enhancing the strengths of features at a level which affects low-dispersion spectral comparison.

As evidence for the blanketing effect of the wind, the high-resolution observations described in Paper I showed that the Mg I 5183 Å line is strongly affected by the shell feature, resulting in more absorption than would be present in a normal supergiant. This shell absorption is almost certainly responsible for the extra Mg I $\lambda5200$ absorption seen in our spectrum divisions (in the supergiant as well as in the disk model ratios).

Part of the downturn below 5000 Å in the spectral division may be due in part to extra line blanketing provided by the wind. Shell components are much weaker in V1057 Cyg (Croswell, Hartmann, and Avrett 1987), so it is not surprising that V1057 Cyg is better matched by the simple disk model.

In summary, simple disk models do a good job in matching the broad-band energy distributions of FU Ori and V1057 Cyg, using only three adjustable parameters: A_V, T_{max}, and the emitting area. Disk models provide better representations of the optical spectrophotometry of V1057 Cyg than do single standard stars. The disk model does very little better, but certainly no worse, than standard stars in matching the optical FU Ori data, and certainly accounts for the optical energy distribution better than supergiants consistent with spectral typing. High-resolution blue spectra can test our suggestion that the shell component significantly blankets the blue spectrum of FU Ori.

d) *Variation of Spectral Type with Wavelength*

Herbig (1977) estimated later spectral types for V1057 Cyg from red spectrograms than from blue spectra. The disk model predicts a similar change in spectral type with wavelength. In Table 5 we present a variety of line indices suggested by O'Connell (1973), with the corresponding spectral types that would be inferred for supergiants using O'Connell's calibration. The synthesized disk indices suggest spectral types in rough agreement with Herbig's (1977) result for V1057 Cyg. We caution that Na I and Mg I absorption in FU Ori (and Na I absorption in V1057 Cyg) is strongly enhanced by the wind, so any agreement between model and observation for these indices is fortuitous. Nevertheless, Table 5 gives some feeling for the kind of wavelength dependence of spectral type that might be inferred from higher resolution observations of other spectral lines.

The detection of M-type photospheric features in the near-infrared (Mould *et al.* 1978; Papers II and III) suggests that TiO features might be visible on optical spectra. The TiO index formally determined from our models is ~ 0.03, corresponding to a mean K3 spectral type (O'Connell 1973). This index

TABLE 5

VARIATION OF SPECTRAL TYPE WITH WAVELENGTH IN FU ORI AND V1057 CYG

Object	Spectral Feature	Absorption Index[a] (spectral type) Predicted	Observed
V1057 Cyg	CN $\lambda3860$	−0.10 (F3 I)	0.02 (F5 I)
	CH $\lambda4305$	0.13 (F3 I)	0.16 (F4 I)
	Mg I $\lambda5175$	0.10 (F8 I)	0.10 (F8 I)
	Na I $\lambda5892$	0.08 (G2 I)	0.10 (G4 I)
	TiO $\lambda7050$	0.05 (<K3)	0.02 (<K3)
FU Ori	CN $\lambda3860$	−0.17 (F2 I)	0.09 (F7 I)
	CH $\lambda4305$	0.11 (F2 I)	0.15 (F3 I)
	Mg I $\lambda5175$	0.10 (F8 I)	0.12 (G2 I)[b]
	Na I $\lambda5892$	0.08 (G2 I)	0.15 (G7 I)[b]
	TiO $\lambda7050$	0.05 (<K3)	0.03 (<K3)

[a] Indices are in magnitudes, as defined by O'Connell 1973.

[b] The Mg I and Na I indices are compromised by mass loss in FU Ori, resulting in a later spectral type than is really appropriate.

assumes that the disk annuli with $T_d \lesssim 3500$ K radiate as blackbodies. This method underestimates the TiO contribution to the optical spectrum; on the other hand, the total flux contribution is lower than the blackbody estimate because of the neglect of blanketing.

We have computed a more realistic TiO index as follows. We adopt the TiO index–spectral type calibration derived by Kenyon and Fernández-Castro (1987), and assume that disk annuli with $T_d \lesssim 3000$ K have TiO band strengths comparable to those of M6 giants. (TiO bands saturate at later types according to White and Wing 1978.) The spectrophotometric observations described by Kenyon and Fernández-Castro suggest that the $m_{7400} - K$ color index is ~ 0.2 mag larger for an M star than for the corresponding blackbody. Therefore, we have scaled the continuum weights for the blackbody annuli in Tables 3 and 4 by 0.8 to account for the extra blanketing present in the spectrum. The TiO index computed in this way is ~ 0.05 for FU Ori and V1057 Cyg, as listed in Table 5. The absence of detectable TiO features in the observed spectra, given the signal-to-noise values, is not inconsistent with the disk model.

e) *Summary of Low-Resolution Analysis*

Simple steady state, viscous accretion disk models can account for many properties of the low-resolution energy distributions of FU Orionis objects from ~ 0.35 μm to ~ 10–20 μm, including the blue and infrared excesses and the variation of spectral type with wavelength. The match between theory and observation involves three free parameters; A_V, T_{max} (constrained by the optical spectral type), and the projected surface area $(R_*/R_\odot)^2 \cos i$. The observations require mass accretion rates onto the central T Tauri star of $\dot{M} \sim 10^{-4}\ M_\odot$ yr^{-1} and central star radii of $R_* \sim 4\ R_\odot$ for adopted disk inclinations of $i \sim 45°$ (see § IV below).

The disk model produces a fairly good, detailed match to the optical continuum of V1057 Cyg (Fig. 3), but fails to explain several features observed in FU Ori (Fig. 5). However, the strong absorption features visible in blue IRS spectra of FU Ori may be enhanced by the shell absorption features described by Herbig (1966).

IV. HIGH-RESOLUTION SPECTRAL SYNTHESIS

a) *Disk Spectrum Synthesis*

We synthesized high-resolution infrared and optical disk spectra using the steady accretion disk models developed in the previous section. Each disk annulus independently radiates as a stellar photosphere of the appropriate spectral type. A high-resolution standard star spectrum is assigned to represent each annulus, weighted by the appropriately normalized flux (as listed in Tables 3 and 4).

The line profiles produced by each annulus are assumed to be the convolution of the stellar spectrum with the profile function

$$\phi(\Delta\lambda) = [1 - (\Delta\lambda/\Delta\lambda_m)^2]^{-1/2}, \quad (4)$$

where $\Delta\lambda = \lambda - \lambda_0$ is the displacement from line center and

$$\Delta\lambda_m = \lambda_0[v_{rot}(R) \sin i]/c \quad (5)$$

is the projected displacement due to the rotational velocity v_{rot} of the annulus at radius R. We use standard star spectra observed with the same equipment as the object spectra, so the instrumental profile affects both model and observation equally. The rotational velocities are assumed to vary as $v \sin i(R) \propto R^{-1/2}$. The contributions from all annuli are then added up to produce the synthetic disk spectrum. Once an accretion disk model is chosen by fitting the low-dispersion energy distributions, the weights, spectral types, and *relative* rotational velocities of each annulus are fixed The only free parameter left to be determined is the normalization of the $v \sin i$ distribution.

The appearance of synthetic high-dispersion spectra is sensitive to the rotational velocity scale adopted. We have analyzed the rotation using cross-correlation techniques (see Hartmann *et al.* 1986 for details) rather than spectrum fitting, for several reasons. The infrared spectra of V1057 Cyg and FU Ori are fairly noisy, so fits to individual lines would be quite uncertain. On the other hand, the cross-correlation technique provides a weighted average over many lines, at the same time accounting for line blending. Another advantage of the cross-correlation methods is that the result is sensitive to line shape, but not to line depths, since mean-subtracted object and template spectra are used. This behavior enables us to separate out the effects of rotational velocities, which are essential predictions of the model, from other features, such as line depths, that are sensitive to details of the spectral standard sequence.

The synthesized spectra are cross-correlated in exactly the same way as the object spectra. The normalization of the $v \sin i$ scale is set by matching observed and synthetic optical cross-correlation peak widths. This single normalization parameter then sets the velocity scale for the infrared spectral synthesis.

The standard stars used for the spectrum synthesis are listed in Table 6. The optical "standards" are supergiants, motivated by the optical spectral types of FU Orionis objects (Herbig 1966, 1977) and the low-dispersion spectrum division analysis discussed in § III. Bad weather prevented us from obtaining an extensive grid of infrared stellar spectral standards with the same resolution as used for the FU Orionis objects. The three cool giants used as standards for infrared spectral synthesis listed in Table 6 span a fair range of effective temperature. It appears that the strongly saturated CO line spectrum is not too sensitive to changes in spectral type (Kleinmann and Hall 1986). We acknowledge, however, that a substantial fraction of the 2 μm disk flux comes from regions cooler than 2000 K (Tables 3 and 4), for which we have no adequate stellar standard. (The M6 giant used to model these regions has $T_{\rm eff} \sim$ 3200 K, according to the calibration of Ridgway *et al.* 1980.)

TABLE 6

STARS USED FOR HIGH-RESOLUTION SPECTRAL SYNTHESIS

HD	Spectral Type[a]	Spectra Range[b]	Other Name
	Optical Spectra		
1457	F0 I	F2–F3	...
8992	F6 Ib	F4–F7	...
190323	G0 Ia	F8–G2	...
187921	G5 Ia[c]	G3–G5	SV Vul
12014	K0 Ib	K0–K2	...
11800	K5 Ib	K5–M1	...
14270	M3 Iab	M2–3100 K	AD Per
11094	M5 II–III	2900–900 K	TT Per
	Infrared Spectra		
82381	K3 III	G5–K2	...
60522	M0 III	K5–3100 K	...
18191	M6 III	2900–900 K	...

[a] Spectral types from Jaschek, Conde, and de Siena 1964.

[b] The range of spectral types or temperatures assigned to each star for purposes of synthesizing the disk spectrum (see Tables 2 and 3).

[c] SV Vul is a long-period Cepheid variable whose spectrum ranges from F7 to K0 (Code 1947). At the time our exposure was taken (JD 2,446,717.6), the spectrum appeared intermediate between our G0 Ia and K0 Ib standards.

b) V1057 Cyg

i) *Cross-Correlation Analysis*

One of the fundamental predictions of the disk model is that the observed values of $v \sin i$ should decrease as the wavelength of observation increases, because at longer wavelengths one observes the outer regions of the Keplerian disk. Cross-correlation analysis is necessary to evaluate this effect, because the infrared spectra are so noisy and blended.

The $v \sin i$ normalization adopted for V1057 Cyg in Table 3 produces the cross-correlation peaks shown in Figure 6. The infrared cross-correlation peak resulting from the optical $v \sin i$ normalization agrees quite well with the observations. Thus, the observed decline of rotational velocity between 6170 Å and 2.2 μm is accurately predicted by the disk model, subject to the sensitivity afforded by our modest infrared instrumental resolution.

For rapidly rotating objects the *shape* of the cross-correlation peak represents a weighted average of the shapes of the lines in the region under consideration. As discussed above, the simplest models suggest that a rotating flattened disk should exhibit somewhat "doubled" line profiles, and therefore doubled cross-correlation peaks. In Paper II we showed that the peaks for cross-correlations of V1057 Cyg at 6170 Å are generally doubled. The shape of the cross-correlation peak of the synthetic optical spectrum agrees very well with observation, suggesting that the disk model profile reproduces the *average* line-profile shape at 6170 Å quite well.

ii) *High-Resolution Optical Spectrum*

The observed optical spectrum of V1057 Cyg shown in Figure 7 represents data accumulated over 11 different nights spanning two years and three observing seasons. The total exposures on seven of the 11 nights were fairly comparable, between $\sim$900 and 2000 photon counts per pixel, and these seven nights comprise about 80% of the total counts. Therefore, the observed spectrum in Figure 7 and the corresponding cross-correlation in Figure 6 represent *time-averaged* observational results for V1057 Cyg.

The synthetic disk spectrum shown in Figure 7 exhibits several doubled line profiles ($\lambda\lambda$6142, 6152, 6170) which are observed in the V1057 Cyg data. In two regions, 6155 and 6168 Å, pairs of lines in the nonrotating spectra are turned into triplets by the superposition of the disk profile peaks, and similar structure is observed in V1057 Cyg. Structure suggestively similar to the disk model is seen in several other features.

To make a clearer test of the disk model predictions, we synthesized the expected spectrum of a uniform, spherical rotating star for comparison, using methods described by Hartmann *et al.* (1986). The disk model does a much better job of accounting for the structure seen in many regions of the high-resolution spectrum than does the uniform rotating star, even in heavily blended regions such as 6147–6150 Å. In general, the disk model produces "sharp" line features in better agreement with observation, while the uniform rotating star produces fairly "rounded" lines and blends. Apparently, the doubled cross-correlation peak for V1057 Cyg (Fig. 6) results from the effects of many lines in this spectral region.

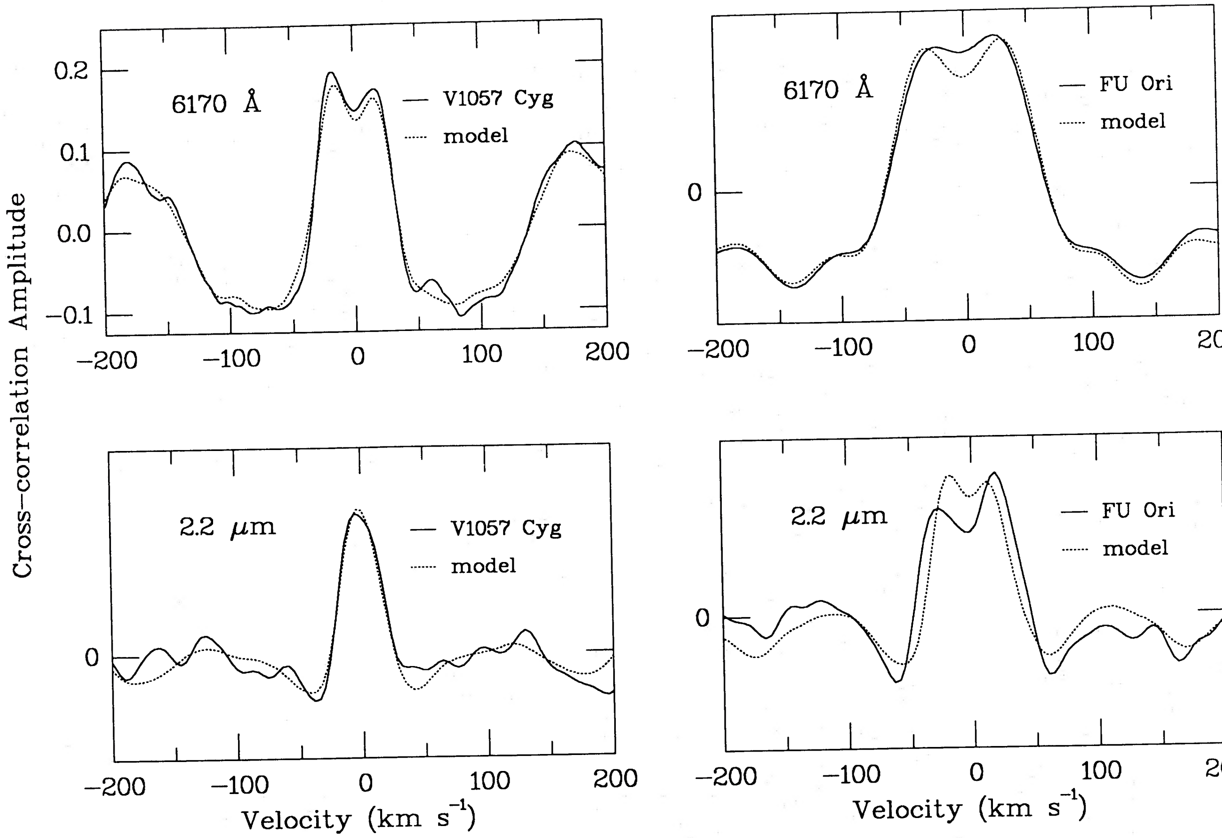

FIG. 6.—Cross-correlation analysis of rotation in FU Orionis objects. *Upper left*: The observed cross-correlation of V1057 Cyg for the echelle order at 6170 Å, compared with the disk model prediction (using Tables 3 and 6). The $v \sin i$ normalization given in Table 3 has been chosen to reproduce the observed cross-correlation peak width. The double structure in the observed peak is accurately reproduced by the model. *Lower left*: Comparison of observed and model infrared cross-correlation peaks for V1057 Cyg. The $v \sin i$ normalization chosen to match the optical data reproduces the observed infrared rotation quite well subject to the modest instrumental resolution in the infrared (the observed peak is only about 1.5 times wider than the resolution limit). This limited resolution prevents any double structure from appearing in the model cross-correlation. The vertical scale of the model cross-correlation (but *not* the zero point) has been adjusted to match the observed peak height. This procedure is justified because the scale of the normalized cross-correlation is set by the variance of the mean-subtracted spectra, and the data are much noisier than the model. *Upper right*: Comparison of observed 6170 Å cross-correlation for FU Ori with model (Tables 4 and 6) prediction. The model predicts line profiles slightly more doubled than were observed. *Lower right*: Comparison of observed and model infrared cross-correlations for FU Ori. The $v \sin i$ normalization used to obtain the curves at the upper right (see Table 4) produces infrared rotation $\sim$25% smaller than observed.

There are some discrepancies between the predicted and the observed line profiles. One prominent difference is that the Ba II line at 6141.7 Å is not as doubled in the model as observed. Other differences, such as the small doubling predicted for the 6158 Å line, are at levels $\sim$1%–2% of the continuum. The synthesized disk spectrum also has somewhat deeper lines relative to the continuum than the observed spectrum.

To isolate the parameters responsible for various features of the synthetic disk spectrum, we calculated "pseudo"-synthetic disk spectra, in which the disk is assumed to radiate at all annuli as a star of a single spectral type. Figure 8 shows two such pseudo-disk calculations. The depths of the lines depend sensitively on the luminosity class or gravity of the standard star spectra. The atmospheric gravity is not a strong constraint of the disk model, since neither the vertical disk height nor the central mass is well determined. We do not think it worthwhile to adjust the synthesized spectrum for this effect, because there are many reasons to think that disk atmospheres may not be like normal stellar atmospheres. For example, the vertical gravity of a disk atmosphere *increases* with increasing height, and the turbulent velocity field of the disk may well differ from that of a star. We simply conclude that the line depths observed at high resolution indicate a low-gravity atmosphere, in reasonable agreement with expected disk gravities $\log g \sim 1$ (see § III*a*).

The lines in the G5 II pseudo-disk spectrum are much more doubled than the corresponding features in V1057 Cyg. Large line broadening in the G supergiant spectrum causes the double-profile structure to be more smeared out. The appearance of the 6141.7 Å line in the supergiant pseudo-disk calculation is a good example of this effect. Thus, at the rotational velocity of V1057 Cyg, we expect the visibility of double-profile structure to be a sensitive function of the "turbulent" broadening in the atmosphere.

The supergiant pseudo-disk spectrum is little different from the disk model spectrum. While the disk model spectrum is a summation over regions with differing effective temperature, the spectra of G and K stars are so similar in this wavelength region that the contributions from different disk annuli are not very apparent. The double-peaked nature of the rotational broadening profile is clearly the dominant effect producing the appearance of the 6170 Å spectra.

The disk model predicts that cool regions contribute to the optical spectrum, so one might expect to see some evidence for a 6160 Å TiO band head not present in G stars. However, the spectrum synthesis indicates that the TiO band should have a

1988ApJ...325..231K

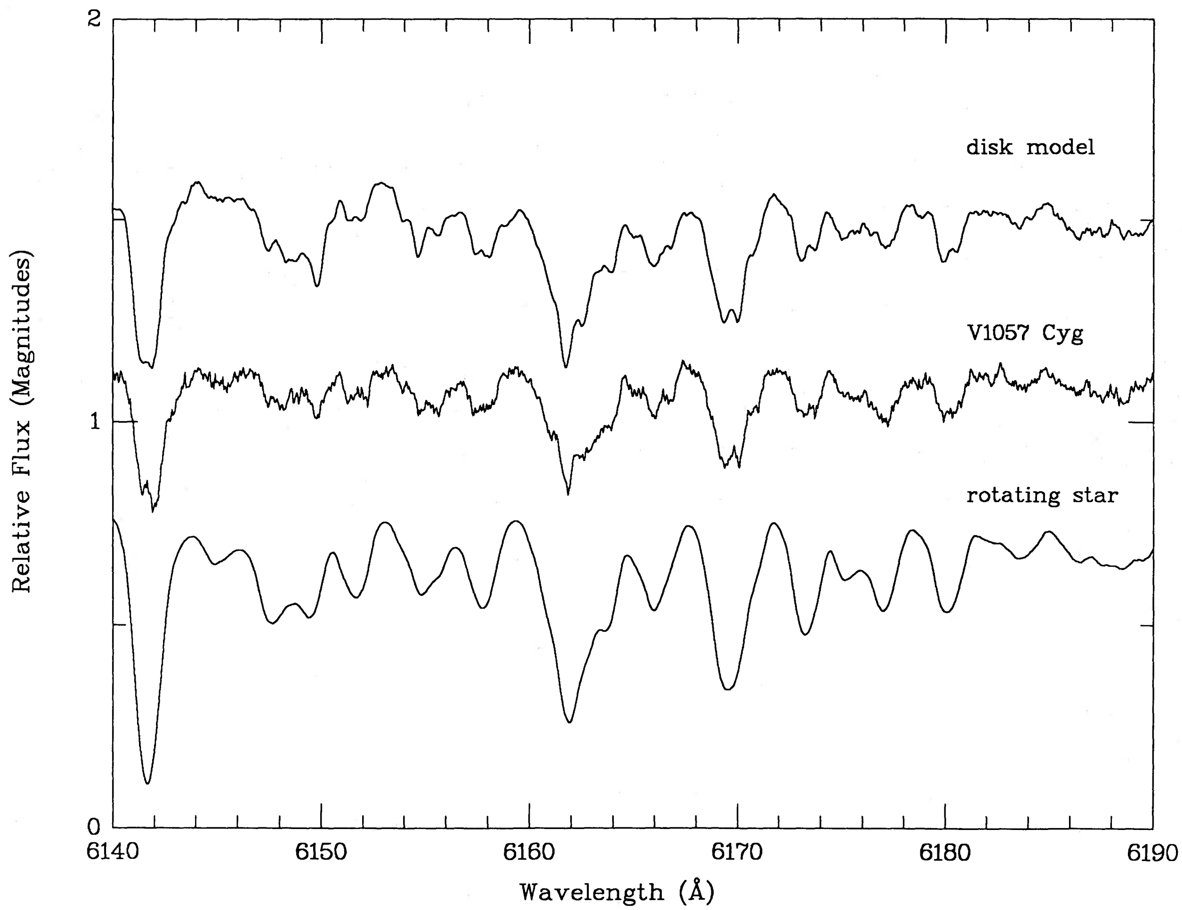

FIG. 7.—High-resolution 6170 Å echelle spectrum of V1057 Cyg compared with the synthetic disk spectrum (*above*) and with the synthesized spectrum of a G5 supergiant rotating at 45 km s^{-1} (*below*).

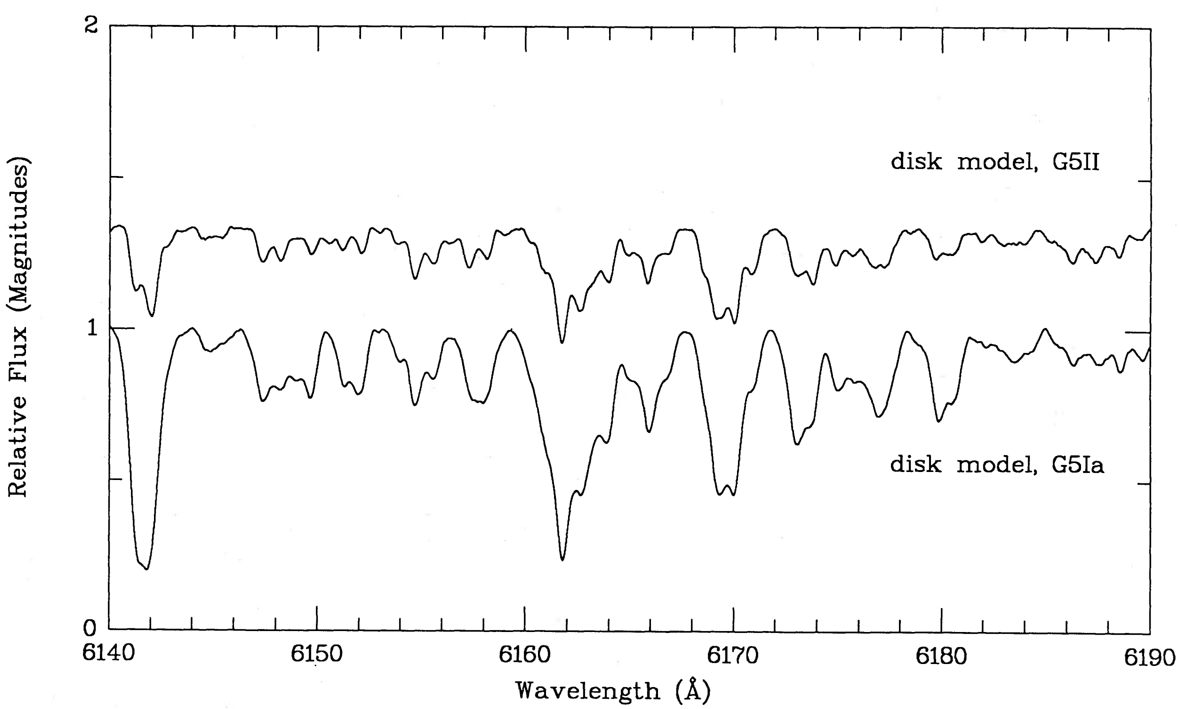

FIG. 8.—A "pseudo"-disk spectrum (see text), in which the disk model weights and rotational velocities in Table 3 are used, but all regions of the disk are assumed to radiate as a star of a single spectral type. The resulting synthesis using the G5 supergiant standard (Table 6) looks very much like the disk synthesis shown in Fig. 7, indicating that the peculiar rotational broadening profile is more important in reproducing the observed spectrum than contributions from regions of differing spectral type. The comparison between G5 I and G5 II "pseudo"-disk models shows that the line depths and doubling of line profiles are sensitive to the luminosity class of the standards used in synthesizing disk spectra.

depth of about 2%–3%. Our spectra are not adequate to find TiO at this level. Distortion in the image-tube package, along with deflection and flexure, changes the position of the echelle orders on the Reticon arrays as a function of telescope position, and is not easily reproducible. These changes in positioning affect the overall shape of the detected spectrum. Although we have attempted to rectify the continuum using polynomial fits, such corrections are probably locally good to no better than 5%. Great care would have to be taken in continuum normalization (i.e., quartz lamps immediately before and after observations, at the same telescope position) to search for effects of TiO λ6160.

iii) *Infrared Spectral Synthesis*

Using the standards given in Table 6, we synthesized an infrared spectrum for the disk model given in Table 3. The synthesized spectrum reproduces the observed depth of the features in the (somewhat noisy) V1057 Cyg spectrum fairly well. This agreement is probably a product of the saturated nature of most of the CO lines, which reduces the dependence of CO equivalent widths on effective temperature and gravity. Certainly M6 III stellar atmospheres are not likely to be good models of the spectra of disk material with $T \sim 1500$ K (Table 3). Problems of the infrared spectral synthesis are discussed in greater detail in the following section on FU Ori. Our analysis indicates that any additional continuum contribution (e.g., dust radiation), which would reduce the depths of the CO lines, must be relatively small ($\lesssim 20\%$).

c) FU Ori

In Figure 6 we exhibit the observed and model cross-correlation peaks for FU Ori. As for V1057 Cyg, the $v \sin i$ distribution has been normalized to produce the same optical cross-correlation peak width.

The observed optical cross-correlation peak is not as doubled as the disk model predicts, although there is some evidence for a departure from the roughly parabolic profile shape expected for a rotating spherical star. The comparison between synthesized and observed optical spectra in Figure 9 shows that the strongest features ($\lambda\lambda$6142, 6162, 6170) are not doubled as predicted. However, several weak features are in much better agreement with the disk model than with a rotating star (most notably the blends at 6146–6150 Å and at 6172–6180 Å). In particular, the appearance of the feature at 6180 Å, which at relevant rotational velocities should appear as a single line (compare the rotating-star spectrum), has a particularly striking doubled appearance. Evidently the shape of the optical cross-correlation peak is a compromise between strong features that *are not* doubled and weaker features that *are* doubled.

The line depths of the synthetic spectrum produced using

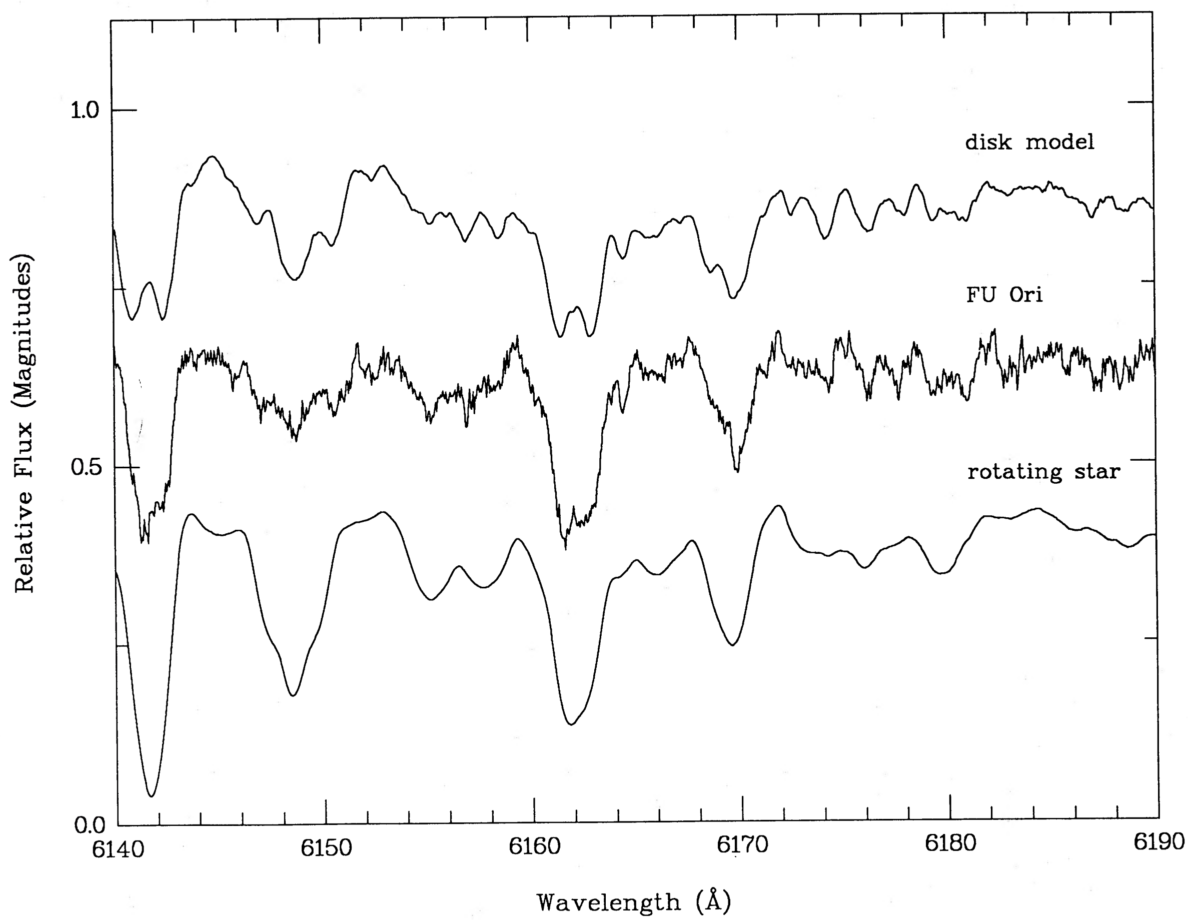

FIG. 9.—High-resolution 6170 Å echelle spectrum of FU Ori compared with the synthetic disk spectrum (*above*) and with the synthesized spectrum of a G5 supergiant rotating at 65 km s^{-1} (*below*).

supergiant spectra are in good agreement with the observed optical lines in FU Ori. Again, as with V1057 Cyg, predicted TiO band contributions are undetectable in our data.

The predicted infrared cross-correlation peak for FU Ori indicates slower rotation at 2.2 μm than at 6170 Å, in qualitative agreement with observation. Quantitatively, the observed infrared cross-correlation peak is about 25% broader than predicted. (It would be difficult to detect a similar discrepancy between observed and predicted infrared rotational velocities in V1057 Cyg, because of its slower rotation and our modest instrumental resolution.) The observed correlation peak for FU Ori is also somewhat more doubled than the predicted peak, although the shapes would agree better if the model rotational velocities were increased.

It is not clear whether the difference between the predicted and observed infrared rotational velocities is significant, because of problems with our standard spectra. One problem is that supergiant standards would match the expected disk gravities better than giants, resulting in somewhat stronger CO lines (see Kleinmann and Hall 1986). And, as mentioned above our M6 III standard spectrum is unlikely to model the coolest disk regions adequately.

A comparison between the observed and synthesized infrared spectra is shown in Figure 10. The overall agreement of line depths is good. The adoption of slightly higher rotational velocities to match the infrared cross-correlation peak width (Fig. 6) reduces the predicted line depths only slightly. As in V1057 Cyg, our results suggest that any additional continuum (dust) contribution to the flux in this region must be $\lesssim 20\%$.

There is some evidence that the disk model lines are not strong enough in the 4310–4350 cm^{-1} interval. This discrepancy may be due to the returning *R*-branch lines of the v'–v'' 2–0 band, which are not saturated in our standard stellar spectra. Note also that the ^{13}CO v'–v'' 2–0 band head in FU Ori at 4264 cm^{-1} is much weaker than in the disk model, showing that FU Ori is not an evolved object (Mould *et al.* 1978).

One indication that the disk calculations do not adequately model the low-temperature regions comes from the strength of water vapor in the 2 μm region. The confluence of many water vapor lines produces strong, broad absorption in the spectra of FU Ori and V1057 Cyg. The spectrophotometry of Mould *et al.* (1978) indicates that water vapor depresses the fluxes at 4900 cm^{-1} relative to the fluxes at 4500 cm^{-1} by $\sim$0.2 and 0.3 mag in FU Ori and V1057 Cyg, respectively. Our FTS standard spectra are not of spectrophotometric quality, owing to cloud conditions, and so cannot be used to estimate water vapor strengths. However, using the standard star atlas of Kleinmann and Hall (1986), we infer that our model using giant stars would result in a 4900 cm^{-1} depression of only $\sim$0.05 mag. The strength of the water vapor features in FU Ori and V1057 Cyg, interpreted in terms of any single star from the Kleinmann and Hall atlas, would seem to require spectral types later than M7 III or M3–M4 Iab.

Carbon (1987) has suggested that blanketing by water vapor lines might reduce the relative strength of the CO lines in very cool atmospheres. Such an effect would reduce the relative contribution of the outermost disk regions to the cross-correlation with CO lines, and would therefore increase the correlation peak width. Carbon's (1987) calculations using crude H_2O opacities for $\log g = 0$ atmospheres show that the H_2O column density above $\tau_{2.3\,\mu m}$ increases by a factor of about 3 relative to that of CO as $T_{\rm eff}$ decreases from 2500 to 2000 K. Since water vapor already strongly depresses the 2 μm continuum in $T_{\rm eff} \sim 3000$ K stars (see Kleinmann and Hall 1986), the contrast of CO absorption lines against the background continuum may be reduced considerably at lower temperatures.

As an experiment, we find that we can reproduce the observed infrared cross-correlation peak width in FU Ori with

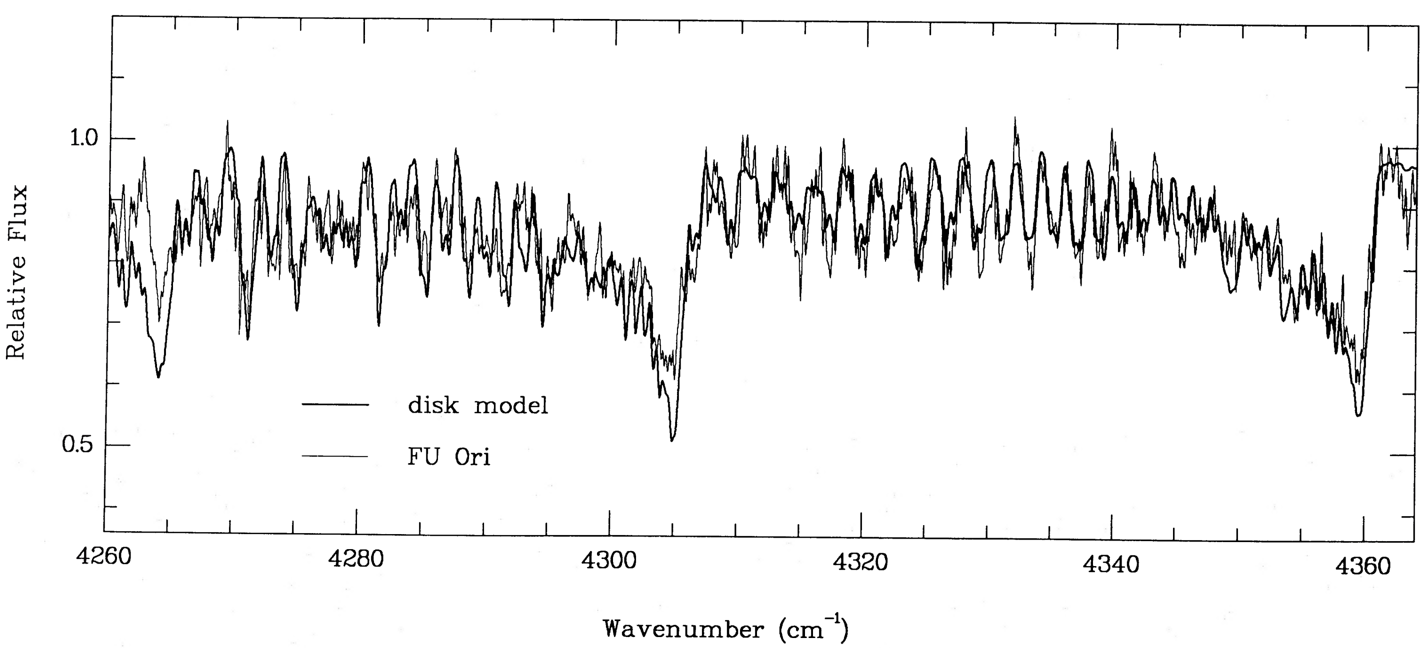

FIG. 10.—High-resolution FTS spectrum of FU Ori compared with the synthesized disk spectrum. The agreement is fairly good, considering the difficulty in using stellar standards for very cool regions (see text). The ^{13}CO band head in FU Ori ($\sim$4265 cm^{-1}) is much weaker than in the evolved giants used for the spectral synthesis.

the same velocity normalization used for the optical spectrum if regions cooler than 2000 K (which account for 29% of the light at *K*) do not contribute to the CO spectrum. More detailed theoretical calculations of very low temperature atmospheres would help indicate the importance of 2 μm H_2O line blanketing.

In the above-mentioned experiment, nearly one-third of the 2 μm light coming from the slowest-rotating regions is thrown away, yet the predicted CO rotational broadening increases by only about 25%. Thus, with any conceivable modification of the standard atmospheres, the model predicts that the infrared rotation *must* be slower than the optical rotation, as observed.

d) Optical Line Profiles, Asymmetries, and Mass Loss

As indicated in Paper I, line doubling in FU Ori and V1057 Cyg is essentially absent in the 5200 Å spectral region. In Figure 11 we compare the average V1057 Cyg spectrum with a disk model synthesized using only a G supergiant spectrum (see discussion of "pseudo"-disk calculations in § IV*b* above). One can see that the synthesized spectrum is far more doubled than the observed spectrum. However, there are two weak lines (at 5186 and 5200 Å) which do appear doubled as predicted, and are significantly different from those expected for a rotating star. Several other features seem intermediate between the disk model and the rotating-star model (λλ5198, 5202, 5204, 5206).

A possible reason for the difference in line profiles between 5200 and 6170 Å is suggested by Figure 12, which presents cross-correlations for the time-averaged spectra. One notes that in both V1057 Cyg and FU Ori, the 6170 Å peaks are fairly symmetric (small deviations being caused by signal-to-noise and template mismatch), while the 5200 Å correlations are strongly asymmetric, with blueshifted peaks. Such asymmetry cannot be produced by the simple disk model, or indeed by any simple axisymmetric static model. We attribute this asymmetry to the strong winds of FU Ori objects, which produce blueshifted "shell" absorption components in strong lines (Herbig 1966, 1977). This interpretation explains why the weakest lines in the 5200 Å spectrum of V1057 Cyg are most similar to the disk model predictions, because these lines should be formed close to the (nonexpanding) photosphere, while the stronger lines are formed farther out in the tenuous, expanding atmosphere. This picture also explains why the cross-correlation peaks are more doubled and symmetric in the red, since the lines in the 5200 Å region are generally much stronger than those in the 6170 Å region. Finally, this mechanism also explains the difference in optical line doubling between FU Ori and V1057 Cyg, since FU Ori has a higher mass-loss rate (Croswell, Hartmann, and Avrett 1987).

We note that the 5200 Å cross-correlation peak in FU Ori appears slightly narrower than the corresponding peak for 6170 Å. The disk model predicts that the rotational velocity

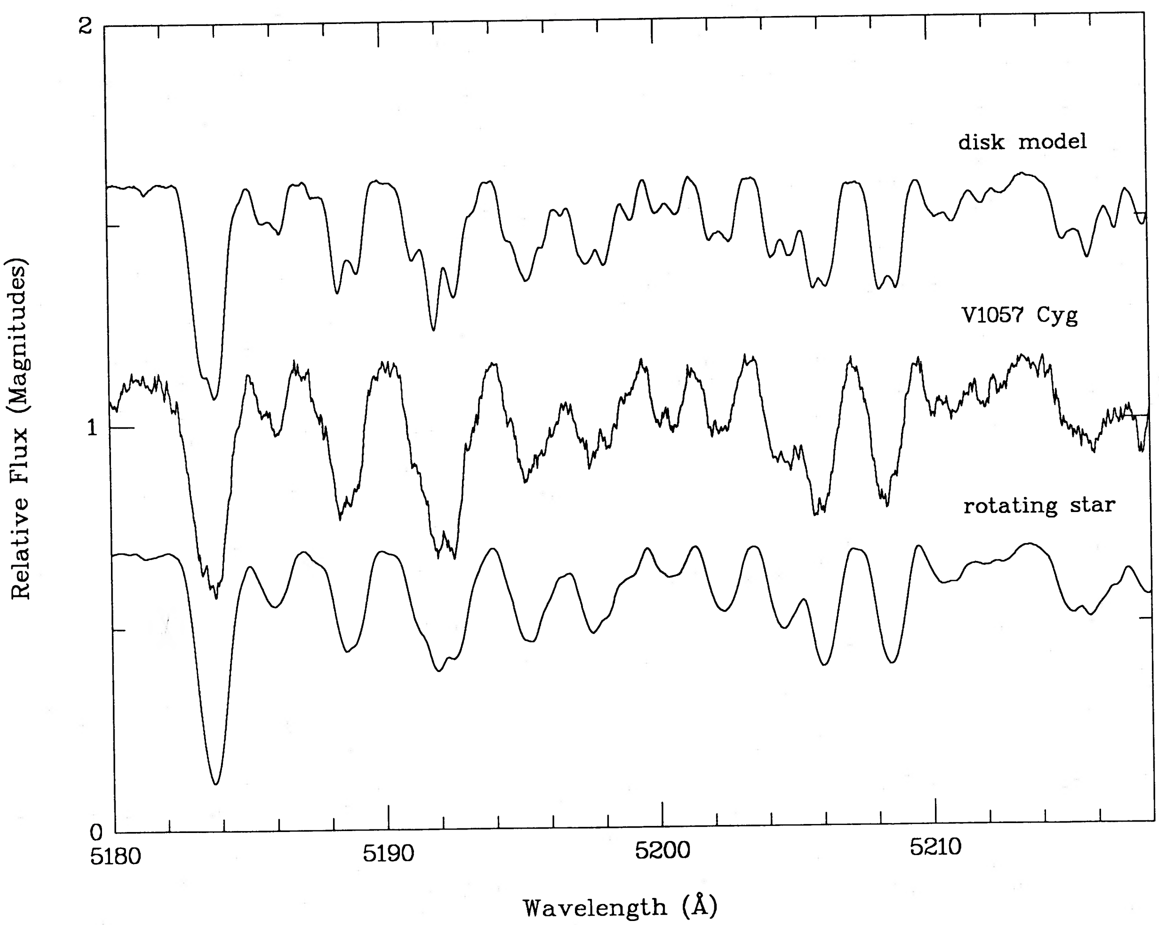

FIG. 11.—Summed V1057 Cyg echelle spectrum near 5200 Å, compared with a pseudo-disk model (above) and a rotating-star model (*below*). The two synthesized spectra use the same G supergiant standard. Most of the lines of V1057 Cyg are not doubled as predicted in this wavelength interval, although two of the weakest lines at 5186 and 5200 Å exhibit striking double structure.

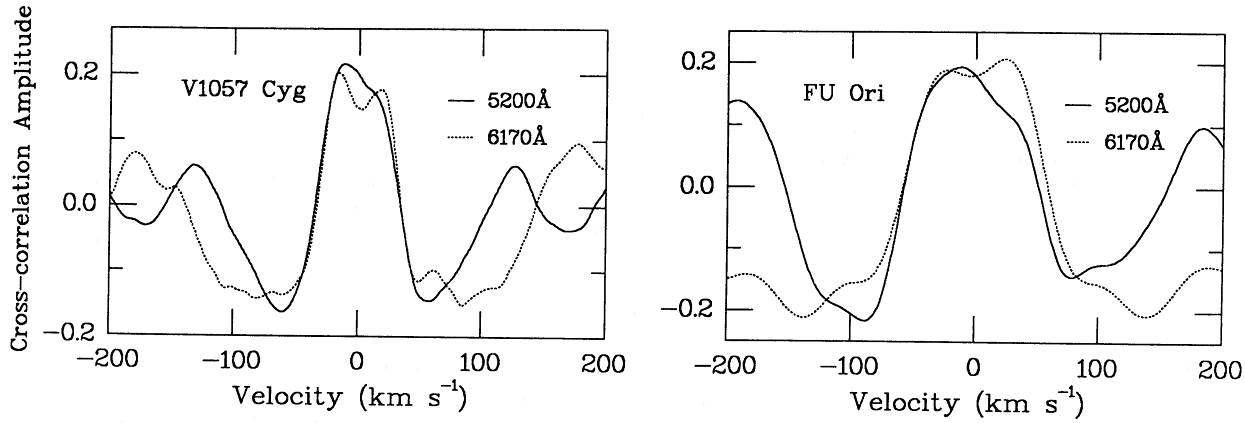

FIG. 12.—Comparison of echelle cross-correlations in two different wavelength regions for V1057 Cyg and FU Ori. The cross-correlations for both objects at 5200 Å are asymmetric, indicating extra blueshifted absorption. We interpret this behavior as the effect of mass loss, which produces larger displacements in the strong lines at 5200 Å than in the relatively weak lines in the 6170 Å region. This effect is likely to obscure any possible line doubling at 5200 Å (see also Fig. 11).

should instead increase with decreasing wavelength. However, the asymmetry of the cross-correlation peak at 5200 Å indicates that line profiles are substantially perturbed by mass loss, making the measurement of line widths problematic in this spectral region.

e) Summary of High-Resolution Synthesis

We conclude that the simple steady accretion disk model reproduces many aspects of high-resolution optical and infrared spectra of FU Ori and V1057 Cyg. The modeling of these properties requires the definition of only one free parameter, $v \sin i\,(R/R_* = 1)$, in addition to parameters already set by fitting the broad-band energy distribution.

The model predicts strong CO absorption features at 2 μm, as observed. The predicted ratio of optical to infrared rotation is in good agreement with observation. The failure of the disk spectrum synthesis to reproduce the strong observed water vapor absorption is probably due to limitations of our standard atmospheres, not to any intrinsic problem of the disk model.

The predicted line profiles for V1057 Cyg are in good agreement with observations at 6170 Å. The comparison between theory and observation is adequate for weak lines in the 6170 Å region for FU Ori. Profiles for lines at 5200 Å in both V1057 Cyg and FU Ori are asymmetric, probably as a result of mass loss.

One should keep in mind that our model spectra are constructed using the simplest possible assumptions, namely, that the disk can be treated as a series of separate standard stellar photospheres. The disk model has tremendously larger lateral velocity shears than are (presumably) present in supergiants, and one could imagine the small amounts of *lateral* (in the disk plane) radiative transfer could broaden line profiles tremendously. Since the predicted line doubling is usually $\sim$10%–20% of the total line depth, modest radiative transfer effects can very easily affect the observed doubling.

V. THE V1057 CYG LIGHT CURVE

The behavior of V1057 Cyg during its decline from visual maximum has important implications for the nature of this luminous object. The published photometry (postmaximum) at V, K, M (4.8 μm), and Q (20 μm) for V1057 Cyg is shown in Figure 13. The decline is a strong function of wavelength for $\lambda \lesssim 3.5$ μm, with a very large decline in the optical ($\Delta U \sim 4$ mag; see Fig. 1 of Kopatskaya 1984; $\Delta V \sim 2.3$ mag), moderate declines at $\sim$1 μm ($\Delta R \sim 2$ mag; $\Delta J \sim 1.3$ mag; Kopatskaya 1984; Rieke, Lee, and Coyne 1972; Simon *et al.* 1982), and a fairly small decline at 3.5 μm ($\Delta L \sim 0.3$–0.4 mag; Rieke, Lee, and Coyne 1972; Grasdalen 1973; Simon *et al.* 1982).

The monotonic fading of brightness for wavelengths between 0.35 and 3.5 μm strongly suggests that *a common source is responsible for the optical and near-infrared emission.* These observations rule out models in which the G-type spectrum in the optical and the M-type spectrum in the near-infrared are produced by two independent sources.

The evolution of V and K in V1057 Cyg resembles that of only three types of eruptive Galactic objects: classical novae (see Payne-Gaposchkin 1957), dwarf novae (see Warner 1976), and symbiotic stars (see Kenyon 1986). Eruptions of novae and some symbiotic binaries are caused by thermonuclear runaways on white dwarf stars (Gallagher and Starrfield 1978; Kenyon 1986; and references therein), and are characterized by an *increase* in effective temperature and the formation of high-ionization emission lines as they decline from visual maximum (Payne-Gaposchkin 1957; McLaughlin 1960). Such phenomena are not observed in the FU Orionis objects, so thermonuclear events have been rejected as the cause of FU Ori eruptions (see Herbig 1966).

Eruptions of dwarf novae and a few symbiotic stars are caused by an increase in the luminosity of a disk surrounding a white dwarf (dwarf novae; Warner 1976) or a main-sequence star (symbiotic stars; Kenyon 1986). Although the reasons for this increase in luminosity are the cause of considerable debate (see Pringle 1981; Smak 1984; Bath 1985), it is well established that the mass accretion rate onto the central object increases as a result of the eruption. The evolution of the decline from visual maximum in these events is characterized by a *decrease* in $\dot{M}$ with time, which causes the disk to become cooler and *the emitted flux to decrease at all wavelengths simultaneously* (see, for example, the discussion of Bath and Pringle 1982 concerning the symbiotic binary CI Cygni, or that of Pringle, Verbunt, and Wade 1986 [and references therein] concerning various dwarf novae). This behavior is consistent with that observed in V1057 Cyg.

By definition, steady disk models do not address the time evolution of accreting systems. Time-dependent hydrodynamic models are needed to make detailed predictions concerning variations in light, and such models are dependent upon

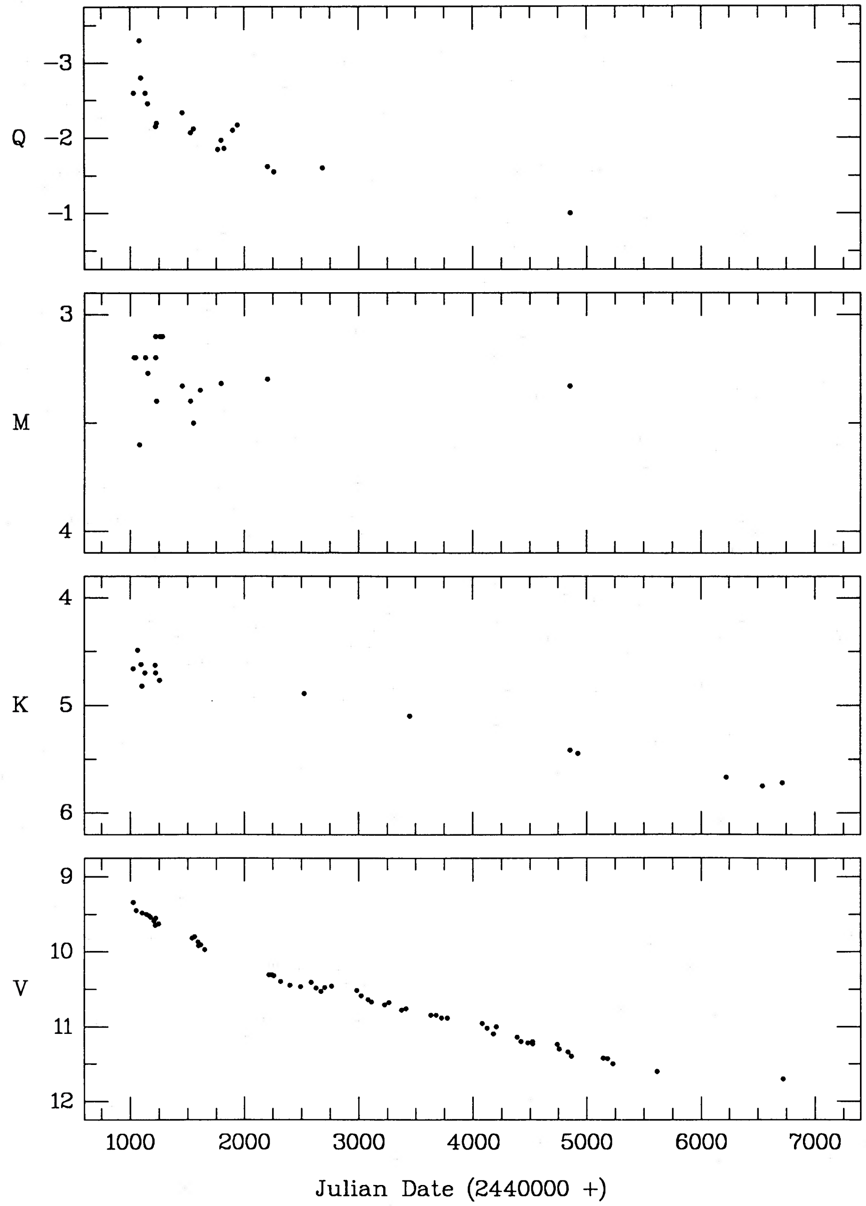

FIG. 13.—Light curves of V1057 Cyg in several photometric bandpasses. Data for the visual light curve were compiled from Lee (1970), Kiselev (1972), Landolt (1975, 1977), Welin (1983), Kopatskaya (1984), and Table 2. Infrared light curves were constructed from data published by Cohen and Woolf (1971), Rieke, Lee, and Coyne (1972), Simon *et al.* (1972), Cohen (1973*a*, 1975), Grasdalen (1973), Simon (1975), Simon and Dyck (1977), Mould *et al.* (1978), Simon *et al.* (1982), and Table 1.

poorly understood viscous processes. However, time-dependent calculations suggest that approximating the decline as a series of steady disks with decreasing $\dot{M}$ is reasonable (but not correct in detail) if the evolution is sufficiently slow (Bath and Pringle 1982). If we adopt our best disk model for V1057 Cyg using 1986 data, then the system would have $M_* \dot{M} \sim 5 \times 10^{-4}\ M_\odot^2\ \mathrm{yr}^{-1}$ near visual maximum when V is $\sim$2.3 mag brighter (see Fig. 13). The optical spectral type of this disk model is ~A5 I, close to the A5 II assigned by Herbig (1977; see also Chalonge, Divan, and Mirzoyan 1982) at visual maximum. The disk model predicts that a 2.3 mag decline in V will be accompanied by declines of 3.6 mag at U, 2 mag at R, and 1.4 mag at K. The observed declines of 4 mag at U, 2 mag at R, and 1.1 mag at K are close to those predicted by the disk model. In view of the obvious difficulties associated with approximating a hydrodynamic event by a series of steady disk models, the agreement between observations and theory is encouraging.

The far-infrared decay in light is considerably greater than would be predicted by simple steady accretion disk models. The 10 and 20 μm fluxes drop by an amount comparable to the optical decay. This behavior suggests that the long-wavelength emission is produced by dust heated by optical radiation from the inner disk.

An optically thick disk with a thickness h which increases with radial distance R intercepts more light from the central star than a thin flat disk, resulting in greater dust radiation in the infrared. In another paper (Kenyon and Hartmann 1987) we suggested that disks around T Tauri stars have $h \propto R^{9/8}$, and that this disk flaring produces enhanced far-infrared fluxes in general agreement with observation. In the present case similar flaring in the outer disk of V1057 Cyg could significantly enhance the dust absorption of radiation produced in inner disk regions, with the result that reprocessing may be more important than accretion at far-infrared wavelengths.

We can estimate the amount of radiation emitted by the inner disk ($R < 10\ R_*$) and intercepted by the outer disk ($R > 100\ R_*$) using the reprocessing disk formalism described by Kenyon and Hartmann (1987). We assume that the intensity of radiation from the inner disk along a given line of sight is proportional to cos *i*, where *i* is measured from the disk's rotational axis to the line of sight. For a disk with $h \propto R^{9/8}$ and $h(R_*) = 0.1\ R_*$, the height of the photosphere at $R \sim 100\ R_*$ is $h/R \sim 0.2$ (SS; Kenyon and Hartmann 1987), so the intensity of radiation intercepted by the outer disk is ~ 5 times smaller than that received by an observer along the disk's rotation axis. If the material with $T \sim 100$–200 K radiates as a blackbody, then the predicted 0.55–20 μm color for the disk model with reprocessing is $V-Q \sim 9$–10 at maximum light, which can be compared to the observed $V-Q \sim 9.3$ for $A_V = 3.5$ mag (Rieke, Lee, and Coyne 1972). The presence of a pronounced silicate peak indicates that the material responsible for the far-infrared flux does not radiate exactly as a blackbody, but the simple reprocessing calculation illustrates that outer regions of the disk can, in principle, provide the observed far-infrared flux without any need for an additional dust cloud.

The only apparent failure of the simple disk model with regard to the evolution of the light curve is the constancy of V1057 Cyg at 4.8 μm. We have no good explanation for this effect Possibly this feature is due to departures of the evolving disk from steady state models.

VI. DISCUSSION

a) Steady Disk Model Predictions

One attraction of the steady accretion disk model is its predictive power. Assuming a normal extinction law, and assuming that the disk radiates as a collection of stellar photospheres, three free parameters—E_{B-V}, $G\dot{M}M_*/R_*$, and $G\dot{M}M_*/R_*^3$—can be chosen to provide a good fit to the spectral energy distributions between 4000 Å and 10 μm. The disk model naturally predicts changes in spectral types as a function of wavelength similar to those observed, and can match the energy distribution of V1057 Cyg between 3500 and 7500 Å to 10%, whereas stellar models match much more poorly. Other models accounting for these effects would surely require additional fitting parameters.

The disk models predict *ratios* of optical to infrared rotational velocities in reasonable agreement with observation without requiring any further free parameters. Using an additional scaling parameter for *v* sin *i*, we find that we are able to account for many peculiar line-profile features in the 6170 Å spectrum of V1057 Cyg, and some features in FU Ori. Not all optical spectral regions show evidence for the disk line-broadening signature (doubled absorption lines), but line shifts due to mass loss clearly limit our ability to detect the subtle disk profile structure.

b) Further Predictions of the Steady Disk Model

The disk model predicts that the spectrum should vary continuously with the wavelength of observation, and therefore the rotational velocity should also vary continuously with wavelength. Unfortunately, this effect will be difficult to verify. The predicted variation of rotation can be estimated rather accurately by computing the variation in half-power radius (i.e., the radius inside which half the radiation at a given wavelength arises as a function of wavelength), and scaling the results by the Keplerian rotation. For example, from Table 3 we find half-power radii of approximately 2.09, 2.29, 2.46, and 3.09 times the inner radius at 5500, 6400 7400, and 9000 Å, respectively; this corresponds to relative rotational velocities of 1.0, 0.96, 0.92, and 0.82 times *v* sin *i* at 5500 Å. Similar results obtain for FU Ori. Thus, unless spectra are available out to nearly 1 μm, predicted optical variations in rotation will be at the level of 10%. Such a small effect may be difficult to detect in competition with possible systematic errors. The expected variation of rotation becomes larger as we proceed to shorter wavelengths, but, as discussed above, there is good evidence that mass loss perturbs the profiles of strong lines commonly present in the blue spectral region. The asymmetric cross-correlation peaks of V1057 Cyg and FU Ori at 5200 Å (Fig. 12) indicate the presence of line-profile effects not explainable as rotation, and presumably the problem of wind or circumstellar shell features will be worse at shorter wavelengths.

Another prediction of the disk model is associated with the variation of rotational velocity with *time*. As the mass accretion rate and the optical flux decrease, the optical radiation becomes more centrally concentrated within the disk and the observed optical rotational velocity should *increase*. If the decline of V1057 Cyg can be approximated by a series of steady disks, then the rotational velocity should increase by 20%–30% from visual maximum to the present epoch. The available data suggest that *v* sin *i* has *decreased* since 1970. Herbig (1977) reported *v* sin *i* $\sim$70 km s^{-1} for metallic lines near visual maximum, while we find *v* sin *i* $\sim$45 km s^{-1} from recent data. However, it appears that the metallic lines are affected by the shell component, because their *radial* velocities decreased from $v_{\rm rad} \sim -50$ km s^{-1} to $v_{\rm rad} = -15$ km s^{-1} during 1971–1973 (Herbig 1977; Fig. 5). Thus we are not able to test predictions involving the time variation of rotational velocity using data near visual maximum.

The disk model adopted for V1057 Cyg in Table 3 predicts a 5%–10% increase in the optical *v* sin *i* for every additional 1 mag decrease in optical brightness, which will be difficult to verify with present technology. The situation is more favorable in the infrared, because the expected increase in *v* sin *i* is about a factor of 2 larger than in the optical ($\sim$10%–15% increase for $\Delta V \sim 1$ mag). Careful infrared observations obtained over the next 10–20 years might be able to test this feature of the disk model.

One might hope to detect TiO features from the M component in the optical. However, as shown in Table 5, the 7050 Å feature will only be a few percent of the continuum at best, and will be blended with atomic lines. The TiO λ8432 band is potentially a more promising feature to search for the M-type photosphere in the optical, because $\sim$30% of the 8500 Å flux in the disk model is emitted by regions with $T_d \lesssim 3500$ K. Unfortunately, the 8432 Å band appears only in M stars with spectral types of M4 and later (Sharpless 1956), and such cool stars contribute only $\sim$15% of the disk flux at 8500 Å. Thus even this TiO feature will be only a few percent deep.

An M-type component must be present in any model, as shown by the 2 μm CO spectrum. A more important test of the continuously varying spectrum prediction would be to find signatures of K stars in the red. The disk model predicts that spectral regions near $\sim$9000 Å should display features characteristic of K supergiants. O'Connell (1973) has shown that the CN band at 9190 Å is much stronger in K1–M1 supergiants than in F2–G2 supergiants, so observations of red CN features might provide another test of the disk model.

Evidence for boundary-layer emission would help support the disk model. Unfortunately, such emission should arise in the ultraviolet, which is very difficult to observe in these heavily reddened objects. There are substantial uncertainties in normal boundary-layer theory (LBP), and the accretion of so much mass onto FU Orionis objects may cause the central star to swell and spin up, reducing the boundary-layer emission considerably. There is some evidence for variability in FU Ori below 4000 Å (§ III*c*, Fig. 4), which in principle could be due to the boundary layer.

c) *Consistency Checks for Accretion Disk Models*

Accretion disk models provide a plausible mechanism for producing the outburst energies and time scales for FU Ori objects (Paper I). Because the viscous dissipation process is not understood, models cannot predict the exact time scales, or account for the time evolution of the spectrum in detail. As shown in Paper I, values of the viscosity parameter $\alpha \sim 0.1$–1 can account for the time scales observed, values which seem at least possible, and are similar to those inferred in other accreting systems (see Bath *et al.* 1974; Bath and Pringle 1982; Cannizzo and Kenyon 1986, 1987; Pringle, Verbunt, and Wade 1986; and references therein).

The rotational velocities are not a constraint in principle, because the disk inclinations are unknown. It would be reassuring if the inner radii and masses for the disk models are consistent with T Tauri parameters for plausible inclinations, since a preoutburst observation of V1057 Cyg suggests a T Tauri spectrum, and one might like to attribute FU Ori outbursts to low-mass pre–main-sequence stars for statistical reasons (Herbig 1977). For a given inclination i, the inner disk radius, R_*, is determined from the model disk luminosity ($\sim R_*^2 \cos i$), and then the mass can be determined from $v \sin i$ at R_*.

In Table 7 we present derived values of radii and masses for FU Ori and V1057 Cyg as a function of inclination. The mass of V1057 Cyg is unreasonably low unless $i < 30°$; some arguments are given by Goodrich (1987) based on the morphology of the nearby reflection nebulosity that this object is observed nearly pole-on. As shown in Table 7, if one assumes that V1057 Cyg has a mass $>0.1\ M_\odot$, then the inferred radius of the central object is $\sim 4\ R_\odot$, comparable to Herbig's (1977) estimate from the preoutburst spectrum, and consistent with the radii of typical T Tauri stars (Cohen and Kuhi 1979).

TABLE 7

DERIVED MASSES AND RADII AS A FUNCTION OF INCLINATION

	V1057 Cyg[a]		FU Ori[a]	
i	$R/R_\odot$	$M/M_\odot$	$R/R_\odot$	$M/M_\odot$
10°	3.77	1.20	3.90	5.97
20	3.86	0.32	3.99	1.57
30	4.02	0.15	4.16	0.77
40	4.27	0.10	4.42	0.49
50	4.66	0.076	4.83	0.38
60	5.29	0.067	5.47	0.34
70	6.40	0.069	6.62	0.35

[a] Estimated errors $\sim \pm 20\%$ in R and M from uncertainties in the distances and in extinction corrections.

For FU Ori one can see that a wide range of inclinations result in reasonable radii $\sim$4–5 $R_\odot$ and masses 1.0–0.4 $M_\odot$. It would not be surprising if the inner radius is slightly larger than T Tauri values, since the accretion of $10^{-2}\ M_\odot$ in the last 50 years might well cause the outer envelope to expand.

We can also investigate the implications of the average observed rotation on the typical masses and inclinations of FU Orionis objects. We include V1515 Cyg, which has an optical rotation roughly half that of V1057 Cyg. We have

$$\langle M_* \sin^2 i \rangle = \langle (v \sin i)^2 R_* \rangle / G\ . \tag{6}$$

Assuming that all three objects have an inner radius $R_* = 4\ R_\odot$, we find $\langle M_* \sin^2 i \rangle = 0.074\ M_\odot$. If one assumes random orientation of axes, the value of $\langle \sin^2 i \rangle = \frac{2}{3}$, which would imply $M_* \sim 0.1\ M_\odot$. This mass is somewhat smaller than one would like for the average T Tauri star. Alternatively, assuming $M_* \sim 0.5\ M_\odot$ would imply $\langle \sin^2 i \rangle = 0.15$. Given the small-number statistics of FU Orionis objects, the discrepancy is not too worrisome. Moreover, the assumption of random orientations cannot be correct. The observed luminosity of a flat disk is proportional to cos i, so there is a selection effect against seeing disks edge-on ($i \sim 90°$). Very young stars may well be surrounded by relatively thick toroids of gas and dust which obscure a finite angle at the rotational equator. We conclude that observations at present are consistent with disk accretion onto T Tauri stars with typical radii and masses.

d) *Other Models*

The strengths of the accretion disk model are even more apparent considering the problems of other explanations. Models in which a G supergiant and an M giant are paired fail to explain the simultaneous decay of optical and near-infrared light in V1057 Cyg, as well as the optical spectral variation with wavelength. Models in which the equatorial regions of a rapidly rotating star produce the near-infrared spectrum fail because the observed infrared rotational velocities are *smaller*, not larger, than the optical rotation.

An alternative model was suggested by Adams, Lada, and Shu (1987, hereafter ALS), in which FU Orionis objects are stars surrounded by disks which reprocess the central star's light. In this model, the optical spectrum is produced by the G supergiant central star, while the infrared spectrum is produced in the disk. As noted in Paper III, the ALS model does not predict any particular ratio of optical to infrared rotational velocities. Our observations show that if the infrared emitting region is rotating at Keplerian velocity, as assumed in both models, then the optical object must also be rotating nearly at breakup. The ALS model also does not account for the complex optical line profiles observed (§ IV), nor does it account for the blue excess (§ III).

Larson (1983) suggested that FU Ori outbursts occur when disk material falls onto the star, causing the outer envelope to expand. In Larson's picture, the central star becomes more luminous because of the energy added by the accreted material. However, the accreted material must radiate roughly as much energy falling in as it can add to the star. This occurs because the kinetic energy of material orbiting at the stellar surface is the same as the potential energy drop the material must pass through (starting at any appreciable distance). Thus, in steady state the disk luminosity is at least as large as the rate of energy deposition to the star, so the accretion-swollen star cannot be more luminous than the disk (just as in simple steady accretion disk models the boundary-layer luminosity is no more than the disk luminosity; LBP). In any reasonable calculation, the swollen star will be considerably fainter than the disk, considering boundary-layer losses and the need to put some energy into expanding the star.

Larson (1983) estimated that accretion of $\sim 10^{-3}\ M_\odot$ could cause the central star in V1057 Cyg to expand by several times its initial radius—if most of the kinetic energy of the accreting material gets transferred to the stellar envelope. It is clearly possible, and even probable, that accretion causes the central stars in FU Orionis objects to expand. However, one would expect that the disk will be much more luminous in the optical for most of the outburst's duration. Furthermore, as discussed above, the observed ratios of optical to infrared rotation imply that the optical component is rotating at nearly breakup. It is difficult to see how accretion of relatively small amounts of mass can cause an object to *expand* into such a rapidly rotating configuration.

VII. FURTHER IMPLICATIONS

a) Accretion Disk Physics

Our results have several interesting implications for accretion disk physics. For example, it is not obvious that the surfaces of such accreting disks should radiate so similarly to stellar photospheres. Depending upon the vertical dependence of viscous dissipation, temperature gradients could be produced that are substantially different from those present in stellar atmospheres (see also Shaviv and Wehrse 1986). The FU Orionis object results indicate that most of the energy is dissipated deep within the optically thick disk.

In § IV we showed that the line profiles in V1057 Cyg at 6170 Å are better fitted with supergiant spectra than with luminosity class II objects. The primary reason for this result is that lines in supergiants are considerably broader than in bright giants. Line broadening in supergiants is poorly understood, but it is usually attributed to a "turbulent" velocity field. The microturbulent velocities required to explain curves of growth in G supergiants are typically ~ 2.5 km s^{-1}, insufficient to account for the observed line widths (e.g., Luck 1977). Luck (1977) estimated a macroturbulent velocity of $\sim 5 \pm 3$ km s^{-1} for the G supergiants ϵ Gem and ϵ Peg, which is comparable to the nearly sonic turbulence implied by viscous disk models with $\alpha \sim 0.1$–1 ($v_{\rm turb} \sim$ a few km s^{-1}). Thus, the line profiles expected from viscous disks can be accommodated by the observations.

The cause of the outburst remains obscure. Disk instability models (e.g., Lin and Papaloizou 1985) remain a possible explanation, but our understanding of viscous processes is so poor that it is hard to make confident predictions. The time duration of FU Orionis outbursts poses a problem; the calculations of Lin and Papaloizou (1985) produced outbursts lasting only $\sim$50–100 days. What this calculation seems to imply is that FU Orionis outbursts start much farther out in the disk than in these models, so that the time scale for decay is much longer. Whether this feature is consistent with disk instability models is not clear.

Another possibility for starting the outbursts, suggested to the authors by A. Toomre, is that FU Orionis objects have stellar companions on eccentric orbits, and that close passage of the companion to the outer disk perturbs the material and begins the eruption.

b) Implications for Stellar Evolution

In Paper II we considered the statistics of FU Ori outbursts, and suggested that, if all low-mass stars undergo such events, they might accrete $\sim 1\%$ of their mass from a disk. The statistics are admittedly quite uncertain. In our calculation we assumed that we have discovered all the FU Ori outbursts that have occurred in the last 80 years within 1 kpc, which should procude a conservative estimate of their frequency. If we have missed some events, as seems likely, the total accreted mass would be revised upward substantially. Obscured FU Orionis objects ought to be luminous ($\sim 10^2\ L_\odot$) *IRAS* sources; searches for such objects could help constrain the frequency of FU Ori outbursts.

The significance of FU Orionis objects may reach beyond direct effects on stellar evolution, by simply demonstrating that *protostellar disk accretion at rapid rates can and does occur.* One might imagine that FU Orionis events represent later stages of disk evolution, where relatively small amounts of material are left in the disk, and winds have had time to clear out lines of sight generally perpendicular to the disk plane (see, for example, the discussion in Adams, Lada, and Shu 1987, and references therein). Disk accretion might be more general and steady in earlier phases hidden by dust, when more material is left in the disk.

We thank the staffs of Kitt Peak National Observatory, the Multiple Mirror Telescope Observatory, and the Whipple Observatory for technical assistance with the various observing runs involved in this project. We also acknowledge useful conversations with G. Herbig, K. Hinkle, S. Kleinmann, D. Lin, J. Pringle, J. Raymond, and J. Stauffer, and thank D. Carbon for computing a sequence of cool model atmospheres at low gravities. This work was supported in part by the Scholarly Studies Program of the Smithsonian Institution.

REFERENCES

Adams, F. C., Lada, C. J., and Shu, F. H. 1987, *Ap. J.*, **308**, 788 (ALS).
Bastian, U., and Mundt, R. 1985, *Astr. Ap.*, **144**, 57.
Bath, G. T. 1985, *Rept. Progr. Phys.*, **48**, 483.
Bath, G. T., Evans, W. D., Papaloizou, J., and Pringle, J. E. 1974, *M.N.R.A.S.*, **169**, 447.
Bath, G. T., and Pringle, J. E. 1982, *M.N.R.A.S.*, **199**, 267.
Cannizzo, J. C., and Kenyon, S. J. 1986, *Ap. J. (Letters)*, **309**, L43.
———. 1987, *Ap. J.*, **320**, 319.
Carbon, D. 1987, private communication.
Carbon, D., and Gingerich, O. 1969, in *Third Harvard-Smithsonian Conf. on Stellar Atmospheres*, ed. O. Gingerich (Cambridge: MIT Press), p. 377.
Chalonge, D., Divan, L., and Mirzoyan, L. V. 1982, *Astrofizika*, **18**, 263.
Code, A. D. 1947, *Ap. J.*, **106**, 309.
Cohen, M. 1973*a*, *M.N.R.A.S.*, **161**, 85.
———. 1973*b*, *M.N.R.A.S.*, **161**, 105.
Cohen, M. 1975, *M.N.R.A.S.*, **173**, 279.
Cohen, M., and Kuhi, L. V. 1979, *Ap. J. Suppl.*, **41**, 743.
Cohen, M., and Woolf, N. J. 1971, *Ap. J.*, **169**, 543.
Croswell, K., Hartmann, L., and Avrett, E. 1987, *Ap. J.*, **312**, 227.
Elias, J. H., Frogel, J. A., Matthews, K., and Neugebauer, G. 1982, *A.J.*, **87**, 1029.
Ewald, R., Imhoff, C. L., and Giampapa, M. S. 1986, in *New Insights in Astrophysics* (ESA SP-263), p. 205.
Gallagher, J. S., and Starrfield, S. G. 1978, *Ann. Rev. Astr. Ap.*, **16**, 171.
Goodrich, R. 1987, *Pub. A.S.P.*, **99**, 116.
Grasdalen, G. L. 1973, *Ap. J.*, **182**, 781.
Hartmann, L., Hewett, R., Stahler, S., and Mathieu, R. D. 1986, *Ap. J.*, **309**, 275.
Hartmann, L., and Kenyon, S. J. 1985, *Ap. J.*, **299**, 462 (Paper I).
———. 1987*a*, *Ap. J.*, **312**, 243 (Paper II).

Hartmann, L., and Kenyon, S. J. 1987*b*, *Ap. J.*, **322**, 393 (Paper III).
Hayes, D., and Latham, D. W. 1975, *Ap. J.*, **197**, 593.
Herbig, G. H. 1966, in *Vistas in Astronomy*, Vol. **8**, ed. A. Beer and K. Aa. Strand (Oxford: Pergamon), p. 109.
———. 1977, *Ap. J.*, **217**, 693.
Herter, T., Lacasse, M. G., Wesemael, F., and Winget, D. E. 1979, *Ap. J. Suppl.*, **39**, 513.
IRAS Point Source Catalog. 1985, Joint *IRAS* Science Working Group (Washington, DC: GPO) (PSC).
Jacoby, G., Hunter, D. A., and Christian, S. 1984, *Ap. J. Suppl.*, **56**, 257.
Jaschek, C., Conde, H., and de Siena, A. C. 1964, *Catalogue of Stellar Spectral Classifications in the Morgan-Keenan System* (La Plata: Universidad Nacional de La Plata).
Kenyon, S. J. 1986, *The Symbiotic Stars* (Cambridge: Cambridge University Press).
———. 1988, in preparation.
Kenyon, S. J., and Fernández-Castro, T. 1987, *A.J.*, **93**, 938.
Kenyon, S. J., and Hartmann, L. 1987, *Ap. J.*, **323**, 714.
Kiselev, N. N. 1972, *Astr. Tsirk.*, No. 742.
Kleinmann, S., and Hall, D. N. B., 1986, *Ap. J. Suppl.*, **62**, 501.
Kolotilov, E. A., and Petrov, P. P. 1985, *Astr. Zh. Pis'ma*, **11**, 846.
Kopatskaya, E. N. 1984, *Astrofizika*, **20**, 275.
Landolt, A. U. 1975, *Pub. A.S.P.*, **87**, 379.
———. 1977, *Pub. A.S.P.*, **89**, 704.
Larson, R. B. 1983, *Rev. Mexicana Astr. Ap.*, **7**, 219.
Latham, D. W. 1982, in *IAU Colloquium 67*, *Instrumentation for Astronomy with Large Optical Telescopes*, ed. C. M. Humphries (Dordrecht: Reidel), p. 259.
Lee, T. A. 1970, *Pub. A.S.P.*, **82**, 765.
Lin, D.N.C., and Papaloizou, J. 1985, in *Protostars and Planets II*, ed. D. C. Black and M. S. Mathews (Tucson: University of Arizona Press), p. 981.
Low, F. J. 1970, *AFCRL Semi-annual Technical Report* (AFCRL-70-0179).
Luck, R. E. 1977, *Ap. J.*, **212**, 743.
Lynden-Bell, D., and Pringle, J. E. 1974, *M.N.R.A.S.*, **168**, 603 (LBP).
Mayo, S. K., Wickramasinghe, D. T., and Whelan, J. A. J. 1980, *M.N.R.A.S.*, **193**, 793.
McLaughlin, D. B. 1960, in *Stars and Stellar Systems*, Vol. **6**, *Stellar Atmospheres*, ed. J. L. Greenstein (Chicago: University of Chicago Press), p. 585.
Mould, J. R., Hall, D. N. B., Ridgway, S. T., Hintzen, P., and Aaronson, M. 1978, *Ap. J.* (*Letters*), **222**, L123.
O'Connell, R. W. 1973, *A.J.*, **78**, 1074.
Payne-Gaposchkin, C. 1957, *The Galactic Novae* (Amsterdam: North-Holland).
Pringle, J. E. 1981, *Ann. Rev. Astr. Ap.*, **19**, 137.
Pringle, J. E., Verbunt, F., and Wade, R. A. 1986, *M.N.R.A.S.*, **221**, 169.
Ridgway, S. T., Joyce, R. R., White, N. M., and Wing, R. F. 1980, *Ap. J.*, **235**, 126.
Rieke, G., Lee, T., and Coyne, G., S. J. 1972, *Pub. A.S.P.*, **84**, 37.
Savage, B. D., and Mathis, J. S. 1979, *Ann. Rev. Astr. Ap.*, **17**, 73.
Schild, R. 1977, *A.J.*, **82**, 337.
Shakura, N. I., and Sunyaev, R. A. 1973, *Astr. Ap.*, **24**, 337 (SS).
Sharpless, S. 1956, *Ap. J.*, **124**, 342.
Shaviv, G., and Wehrse, R. 1986, *Astr. Ap.*, **159**, L5.
Simon, T. 1975, *Pub. A.S.P.*, **87**, 317.
Simon, T., and Dyck, H. M. 1977, *A.J.*, **82**, 725.
Simon, T., Morrison, N. D., Wolff, S. C., and Morrison, D. 1972, *Astr. Ap.*, **20**, 99.
Simon, T., Wolstencroft, R. D., Dyck, H. M., and Joyce, R. R. 1982, *Inf. Bull. Var. Stars*, No. 2155.
Smak, J. 1984, *Pub. A.S.P.*, **96**, 5.
Warner, B. 1976, in *IAU Symposium 73*, *The Structure and Evolution of Close Binary Systems*, ed. P. Eggleton, S. Mitton, and J. Whelan (Dordrecht: Reidel), p. 85.
Welin, G. 1983, *Inf. Bull. Var. Stars*, No. 2423.
White, N. M., and Wing, R. F. 1978, *Ap. J.*, **222**, 209.
Wu, C.-C., *et al.* 1983, *IUE NASA Newsletter*, No. 22.

L. Hartmann, R. Hewett, and S. J. Kenyon: Smithsonian Astrophysical Observatory, Harvard-Smithsonian Center for Astrophysics, 60 Garden Street, Cambridge, MA 02138